MISR overview and observational principles
Data products
Example data applications

David J. Diner
Jet Propulsion Laboratory, California Institute of Technology

Eugene E. Clothiaux
Department of Meteorology, The Pennsylvania State University

Exploring and Using MISR Data
College Park, MD
September 2006

MISR characteristics

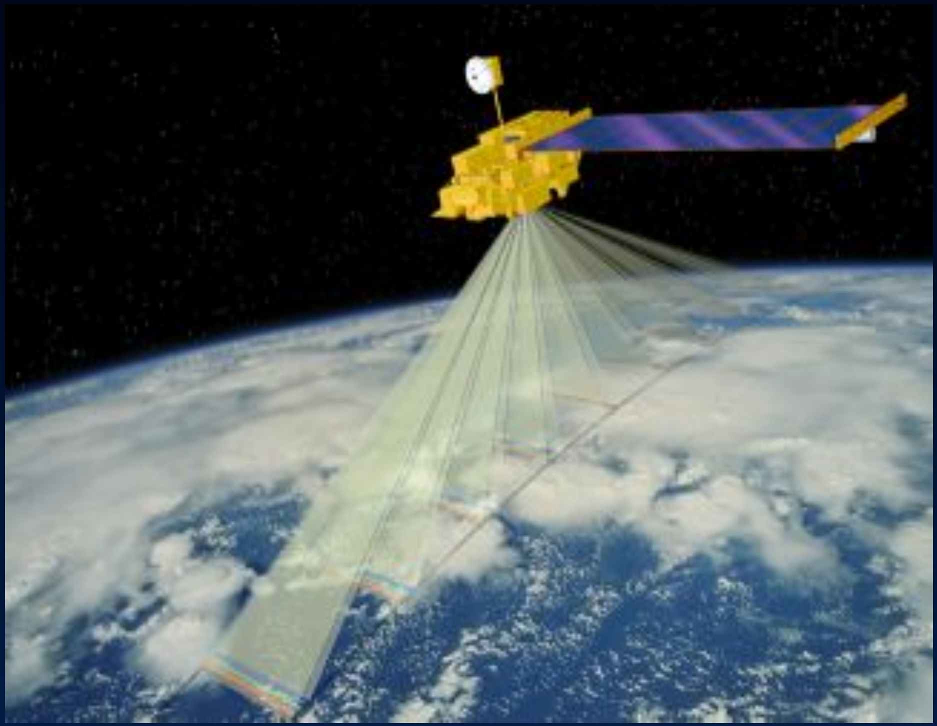

Flies on Terra

9 view angles at Earth surface:
70.5°. 60.0°, 45.6°, 26.1° forward of nadir
nadir
26.1°, 45.6°, 60.0°, 70.5° backward of nadir

Four spectral bands at each angle:
446 nm ± 21 nm
558 nm ± 15 nm
672 nm ± 11 nm
866 nm ± 20 nm

Global Mode (continuous):
275 m sampling in all nadir bands and
red band of off-nadir cameras
1.1 km for the other channels

Local Mode (targeted): 275 m all channels

400-km swath: Complete zonal coverage
9 days at equator, 2 days at poles

14-bit quantization

Radiometrically, geometrically calibrated

Why multi-angle?

1. Change in reflectance with angle distinguishes different types of aerosols, and surface structure

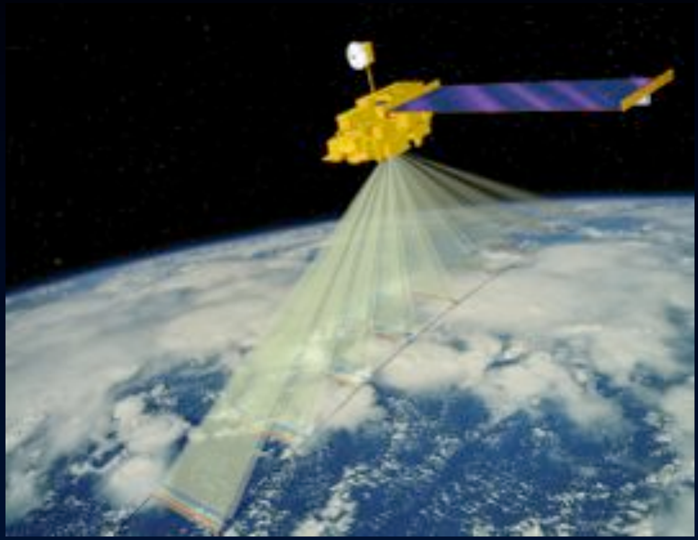

2. Oblique slant paths through the atmosphere enhance sensitivity to aerosols and thin cirrus

3. Stereo imaging provides geometric heights of clouds and aerosol plumes

4. Time lapse from forward to backward views makes it possible to use clouds as tracers of winds aloft

5. Different angles of view enable sunglint avoidance or accentuation

6. Integration over angle is required to estimate hemispherical reflectance (albedo) accurately

MISR instrument

Family portrait

The “V-9” optical bench

Undergoing test

JPL’s Space Simulator Facility

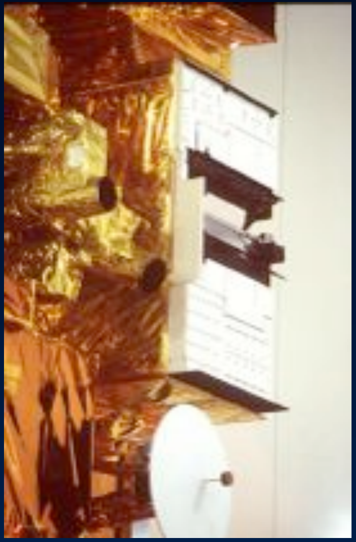

MISR on Terra spacecraft

Terra launch 18 December 1999

MISR calibration

Absolute radiometric uncertainty 3%
Relative radiometric uncertainty 2%
Temporal stability 1%
Geolocation uncertainty 50 m
Camera-to-camera registration < 275 m

MISR On-Board Calibrator

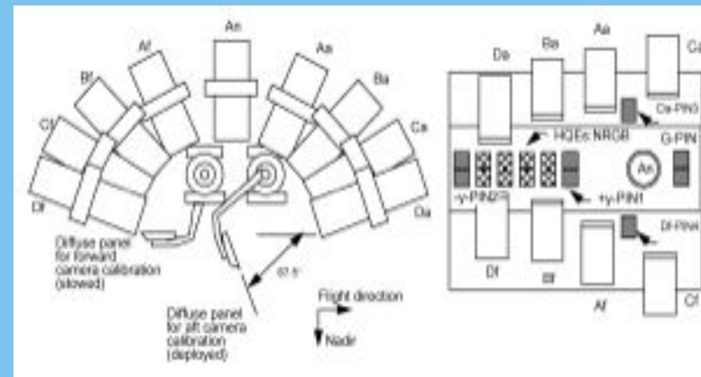




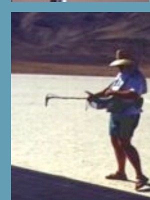


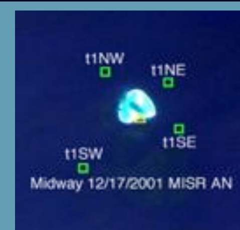

Vicarious calibrations and validations over desert playas and dark water sites


AirMISR

MISR lunar images

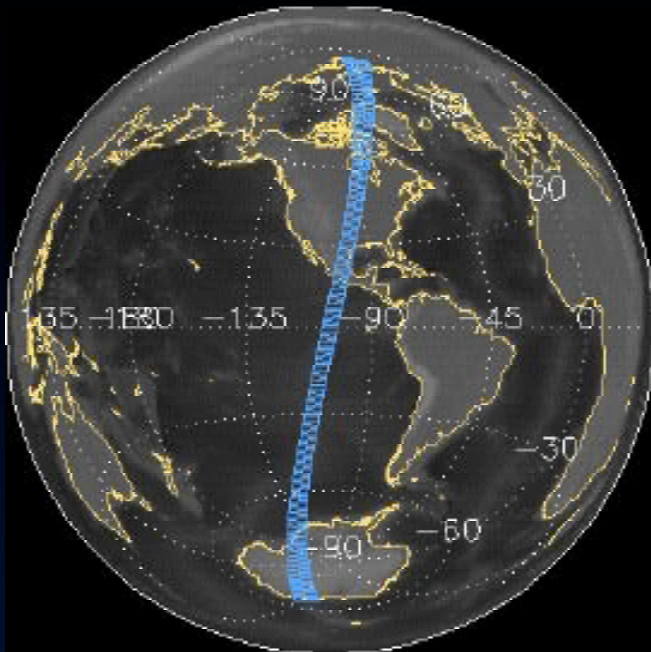

MISR geolocation and angle-to-angle coregistration

Space Oblique Mercator projection minimizes resampling distortions

233 unique paths in 16-day repeat-cycle of Terra orbit

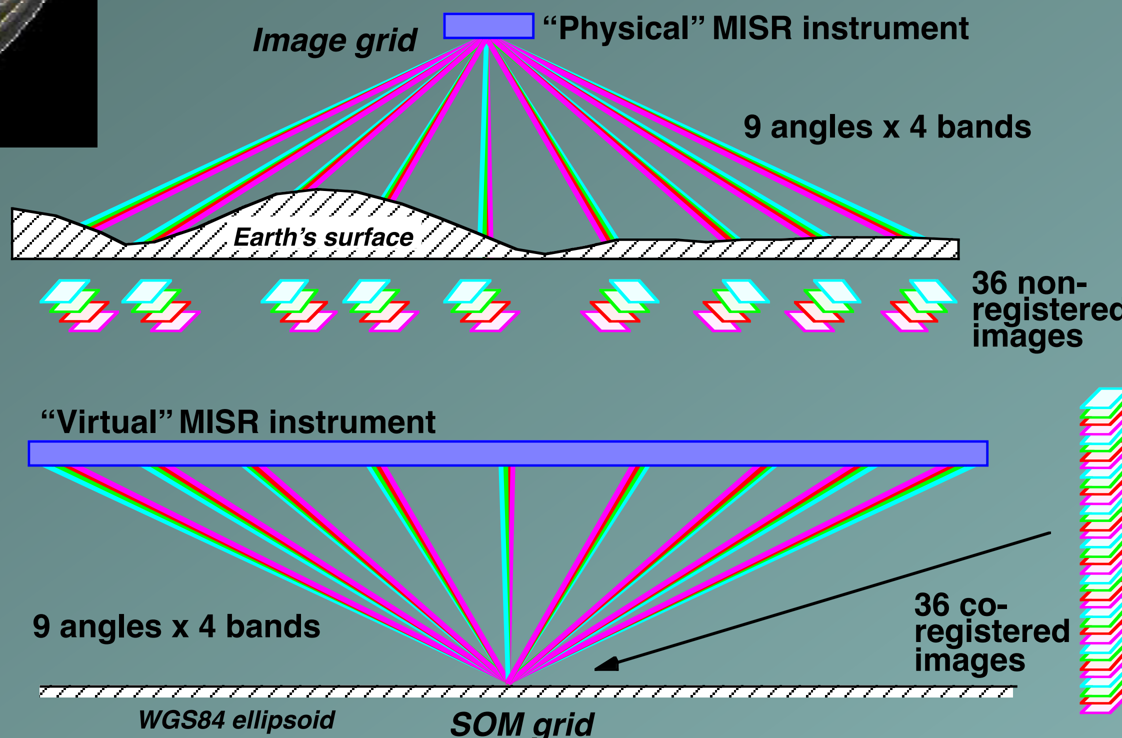

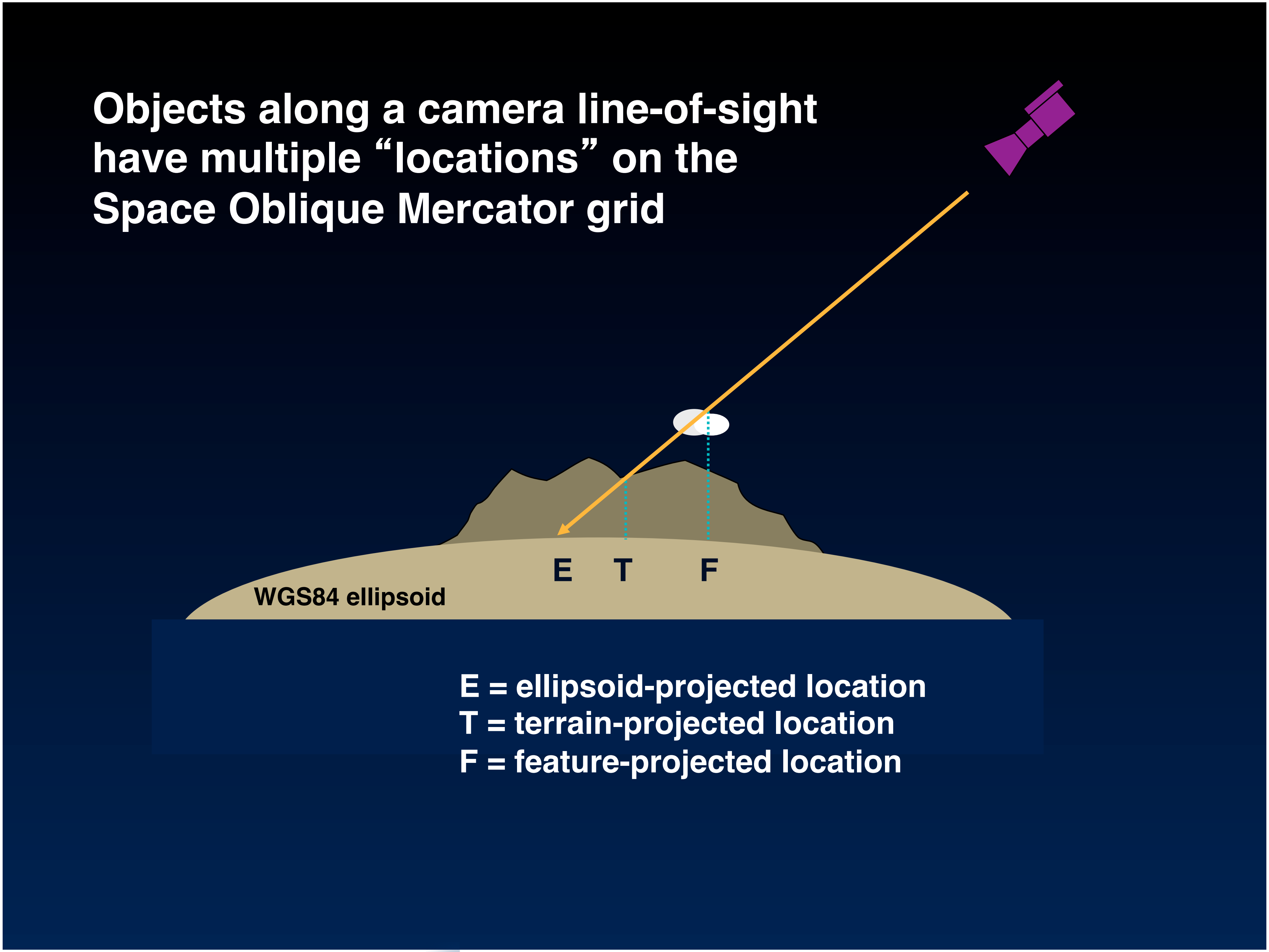
Objects along a camera line-of-sight have multiple “locations” on the Space Oblique Mercator grid
E
T
F
WGS84 ellipsoid
E = ellipsoid-projected location
T = terrain-projected location
F = feature-projected location

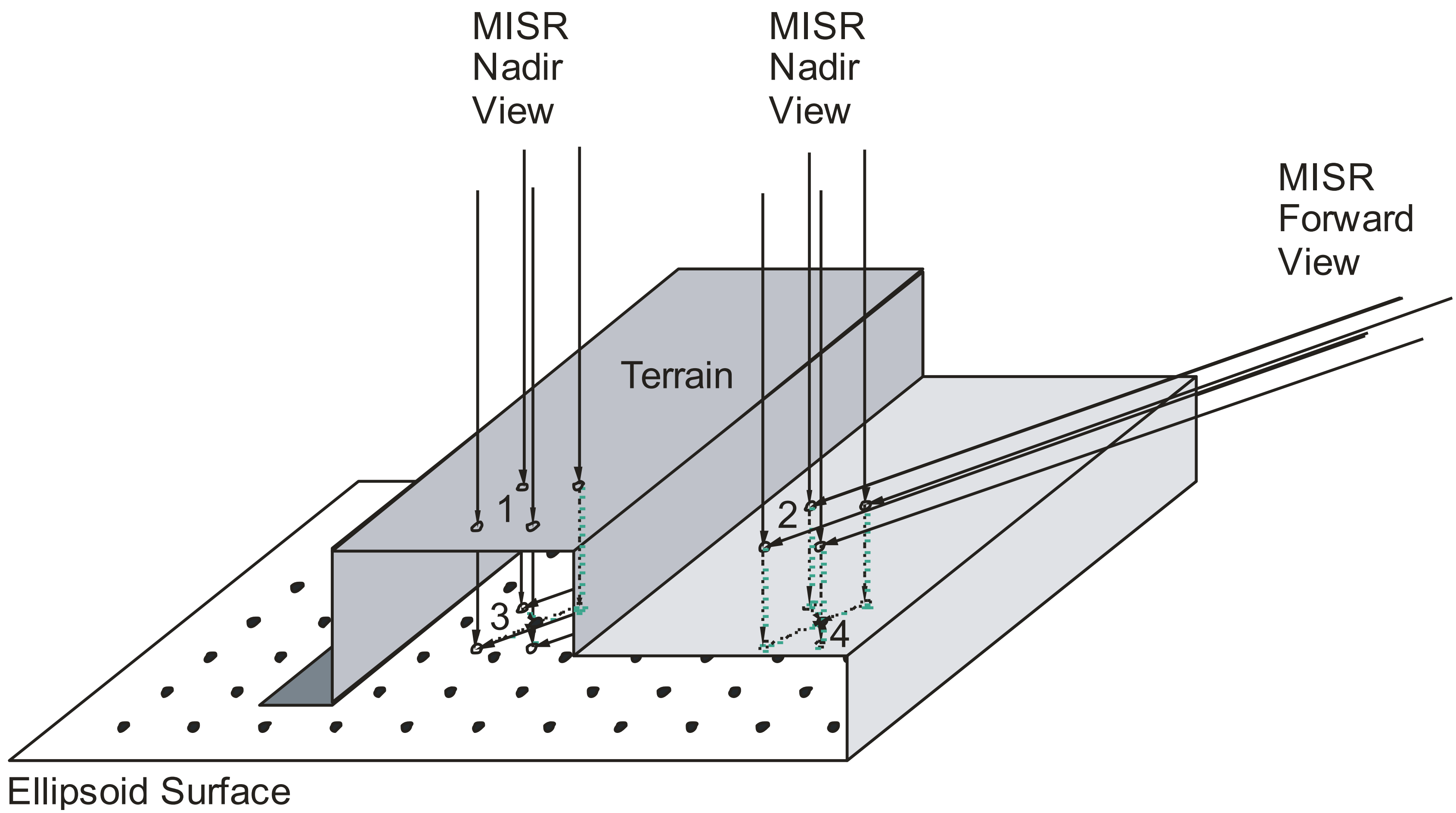
MISR
Nadir
View
MISR
Nadir
View
MISR
Forward
View
Terrain
1
2
3
4
Ellipsoid Surface

AirMISR

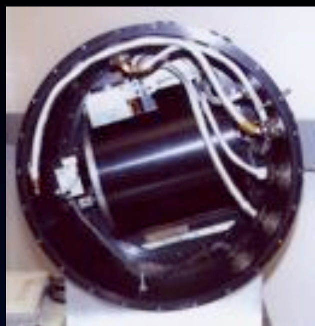

Mounted in nose of NASA ER-2

Covers MISR's nine angles

Uses gimballed MISR prototype camera

27.5 m georectified spatial resolution

9 x 11 km area covered at all angles

Data available at LaRC DAAC

46° images near Howland, ME 28 August 2003

MISR science operations

Global Mode

- Pole-to-pole coverage on orbit dayside
- Full resolution in all 4 nadir bands, and red band of off-nadir cameras (275-m sampling)
- 4x4 pixel averaging in all other channels (1.1-km sampling)

Local Lode

- Implemented for pre-established targets (1-2 per day)
- Provides full resolution in all 36 channels (275-m sampling)
- Pixel averaging is inhibited sequentially from camera Df to camera Da over targets approximately 300 km in length

Calibration

- Implemented bi-monthly
- Spectralon solar diffuser panels are deployed near poles and observed by cameras and a set of stable photodiodes

Level 1 Standard Products

Level 1 standard products

- Level 1A reformatted, annotated product
- Level 1B1 radiometric product
- Level 1B2 georectified radiance product, global and local modes:
  - ellipsoid projected
  - terrain (blocks containing land only) projected
- Level 1B2 browse (JPEG)
- Level 1B2 geometric parameters
- Level 1B2 radiometric camera-by-camera cloud mask

Level 1 processing operates on each camera individually

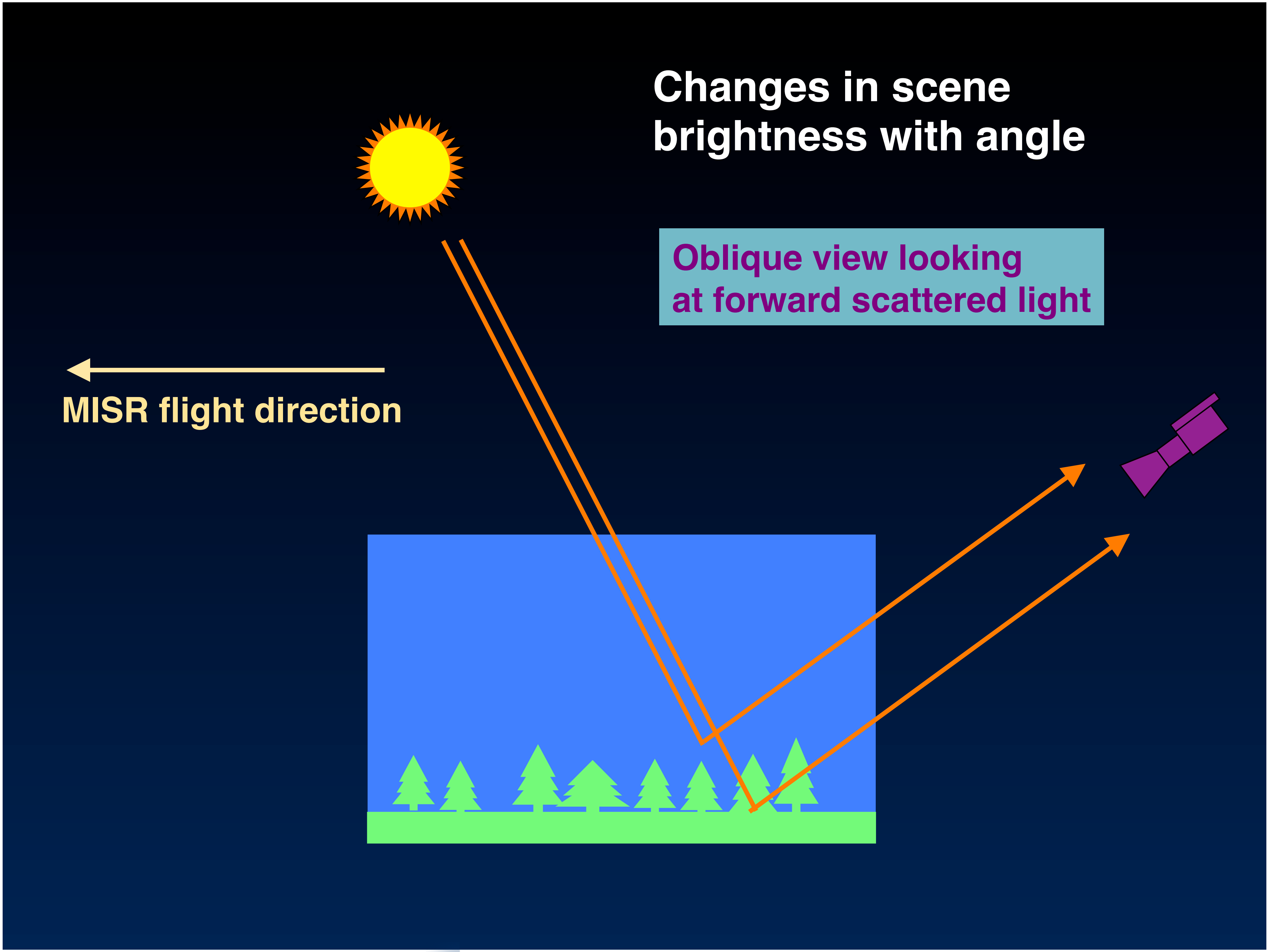
Changes in scene brightness with angle
Oblique view looking at forward scattered light
MISR flight direction

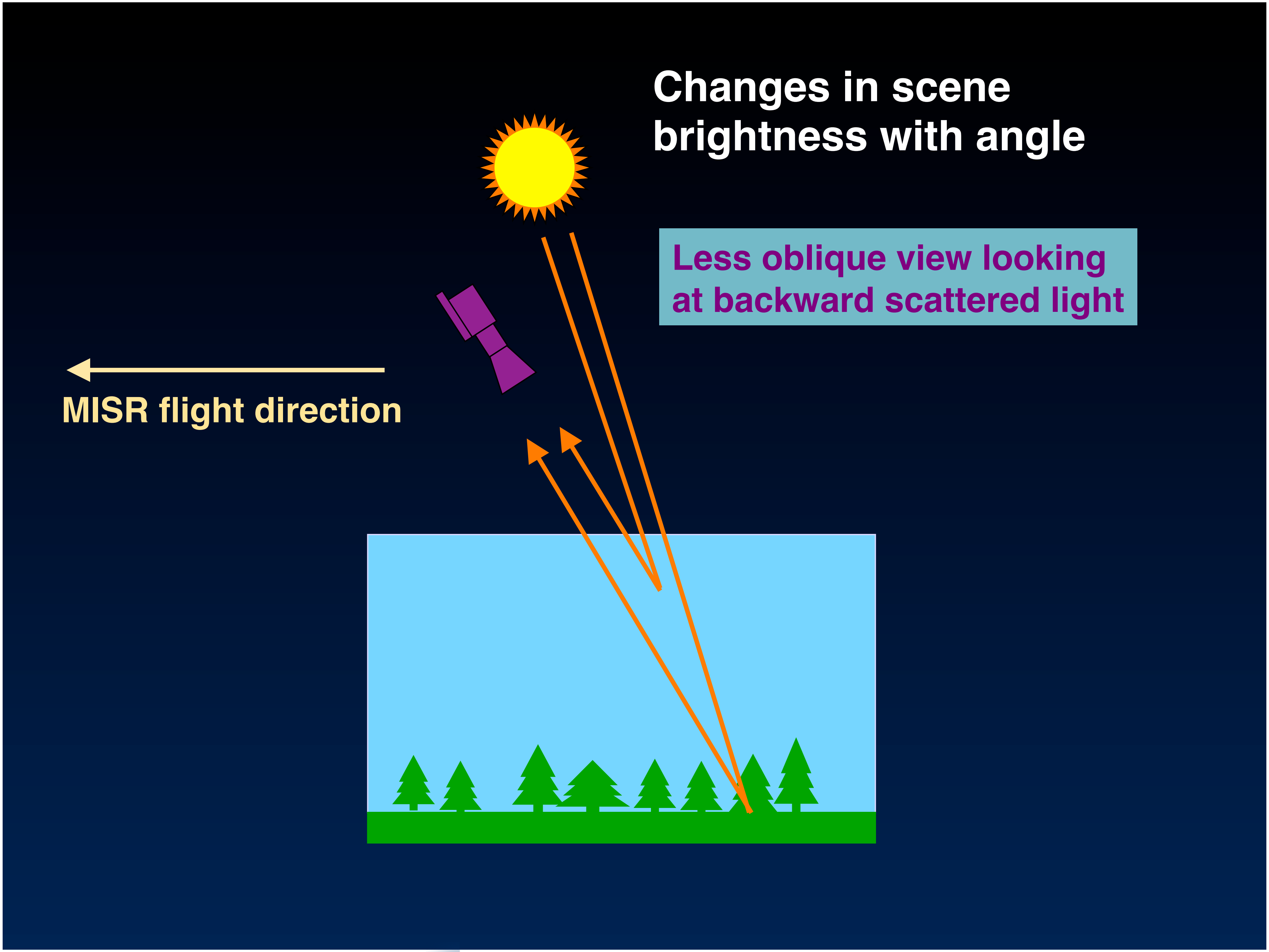
Changes in scene brightness with angle
Less oblique view looking at backward scattered light
MISR flight direction

Visualizing surface texture

multi-spectral compositing

Hudson and James Bays
24 February 2000

nadir blue band | **nadir green band** | **nadir red band**

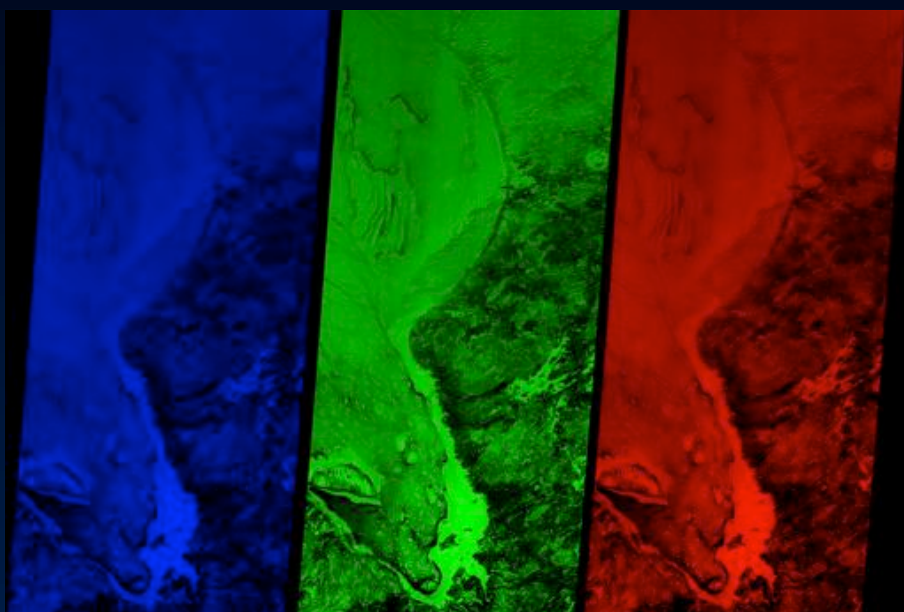

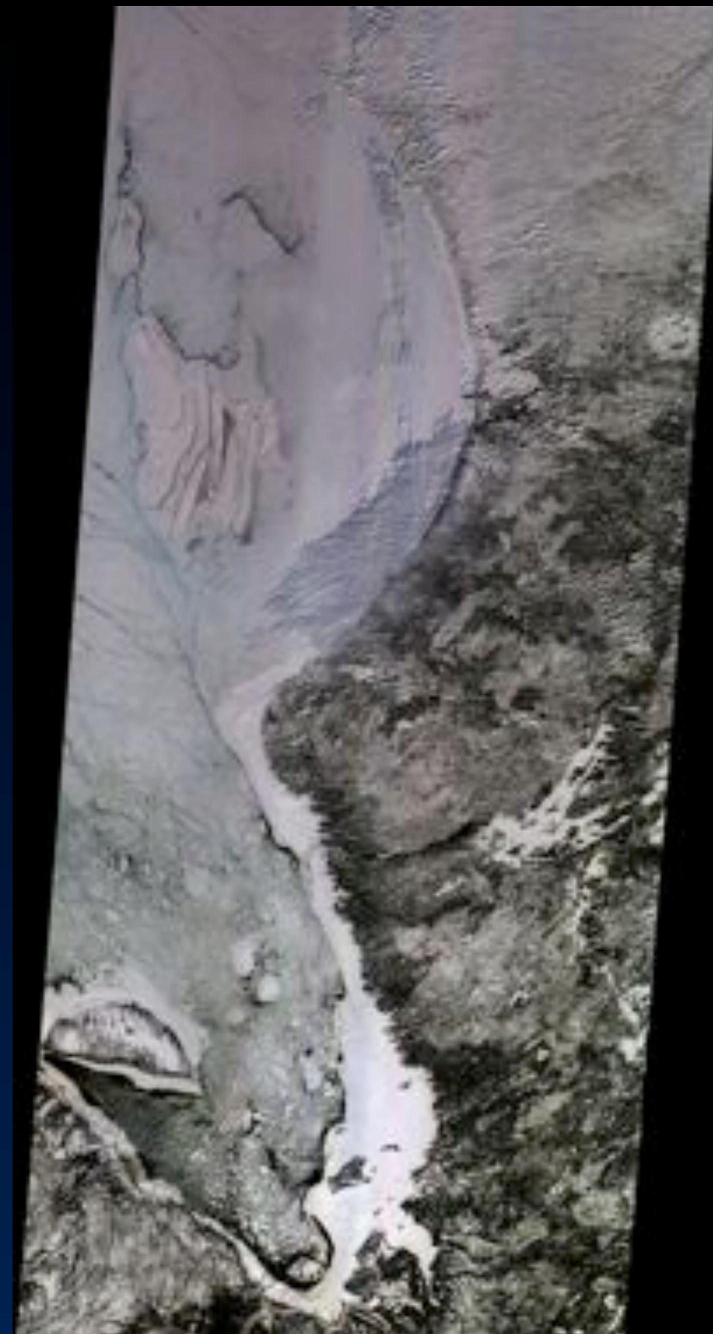

Visualizing surface texture

multi-angle compositing

Hudson and James Bays
24 February 2000

70° forward red band	nadir red band	70° backward red band

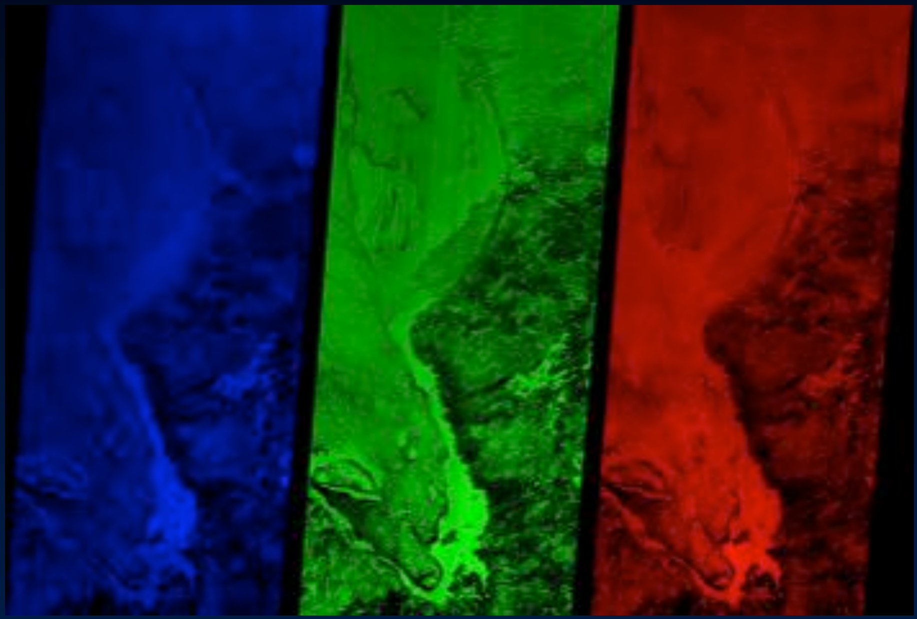

Cloud and ice bidirectional reflectances

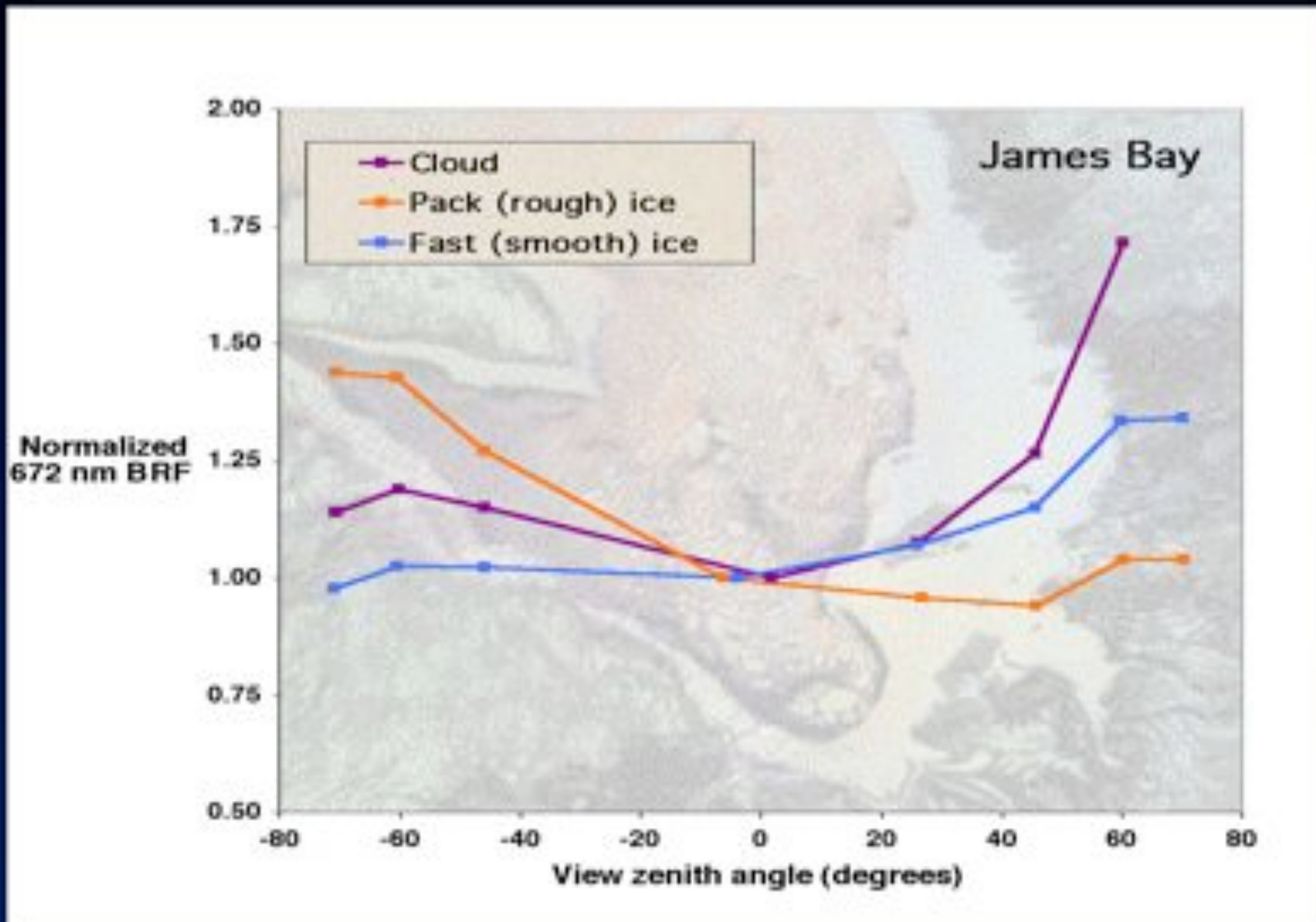

Mapping changes in ice sheet rifts

Amery Ice Shelf "Loose Tooth"

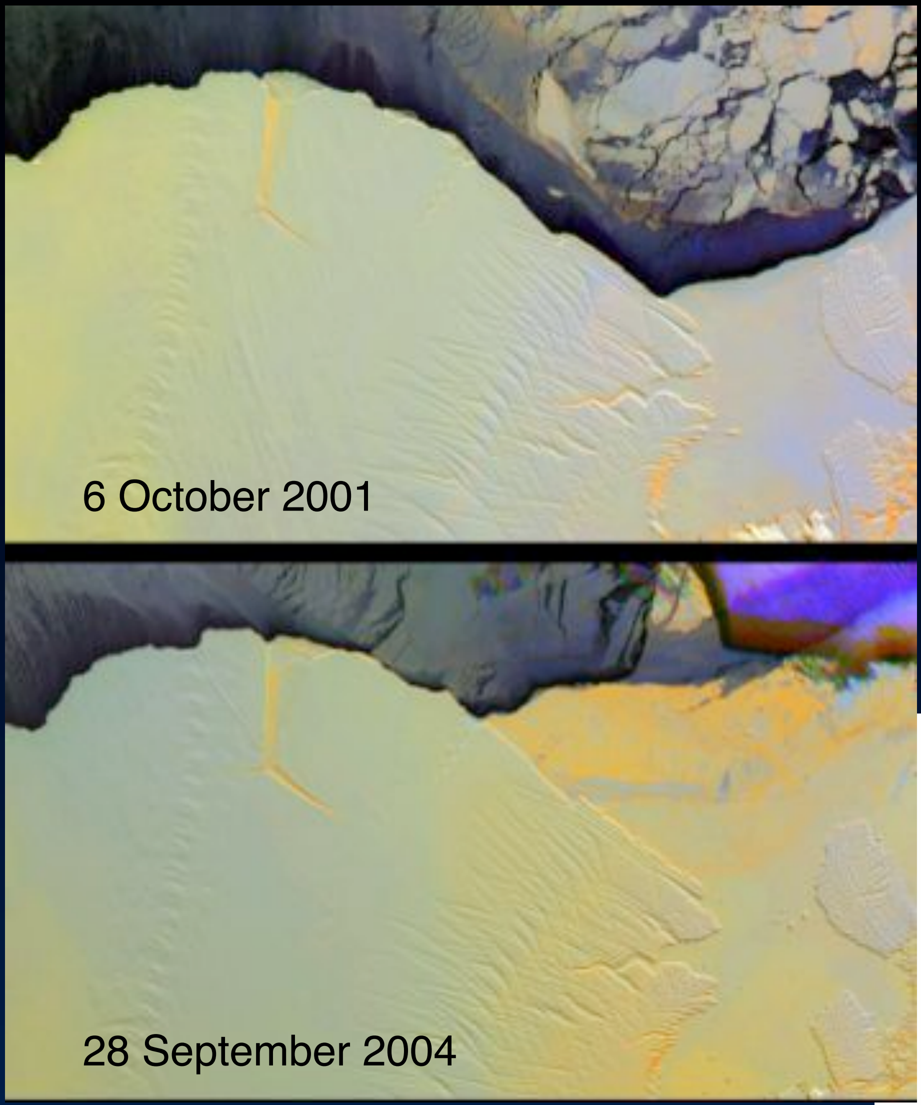

Multiangle red-band composites

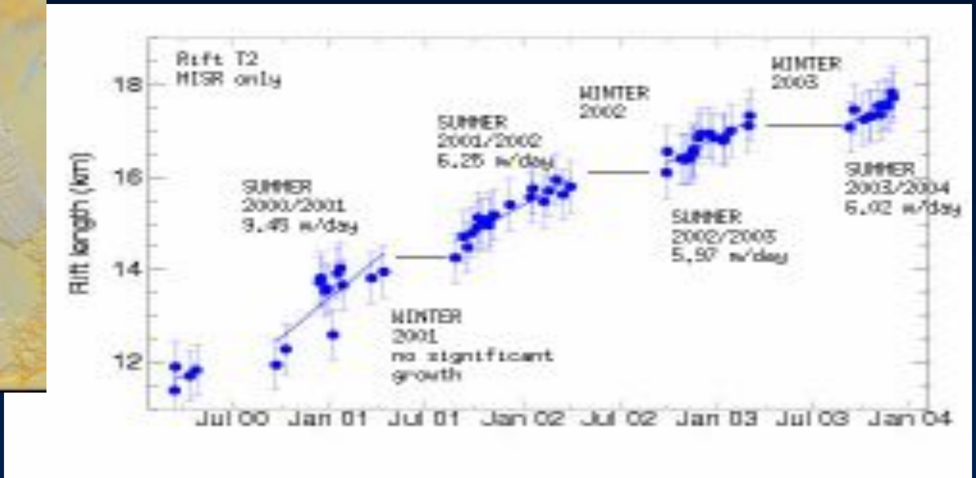

H.A. Fricker et al. (2005), GRL

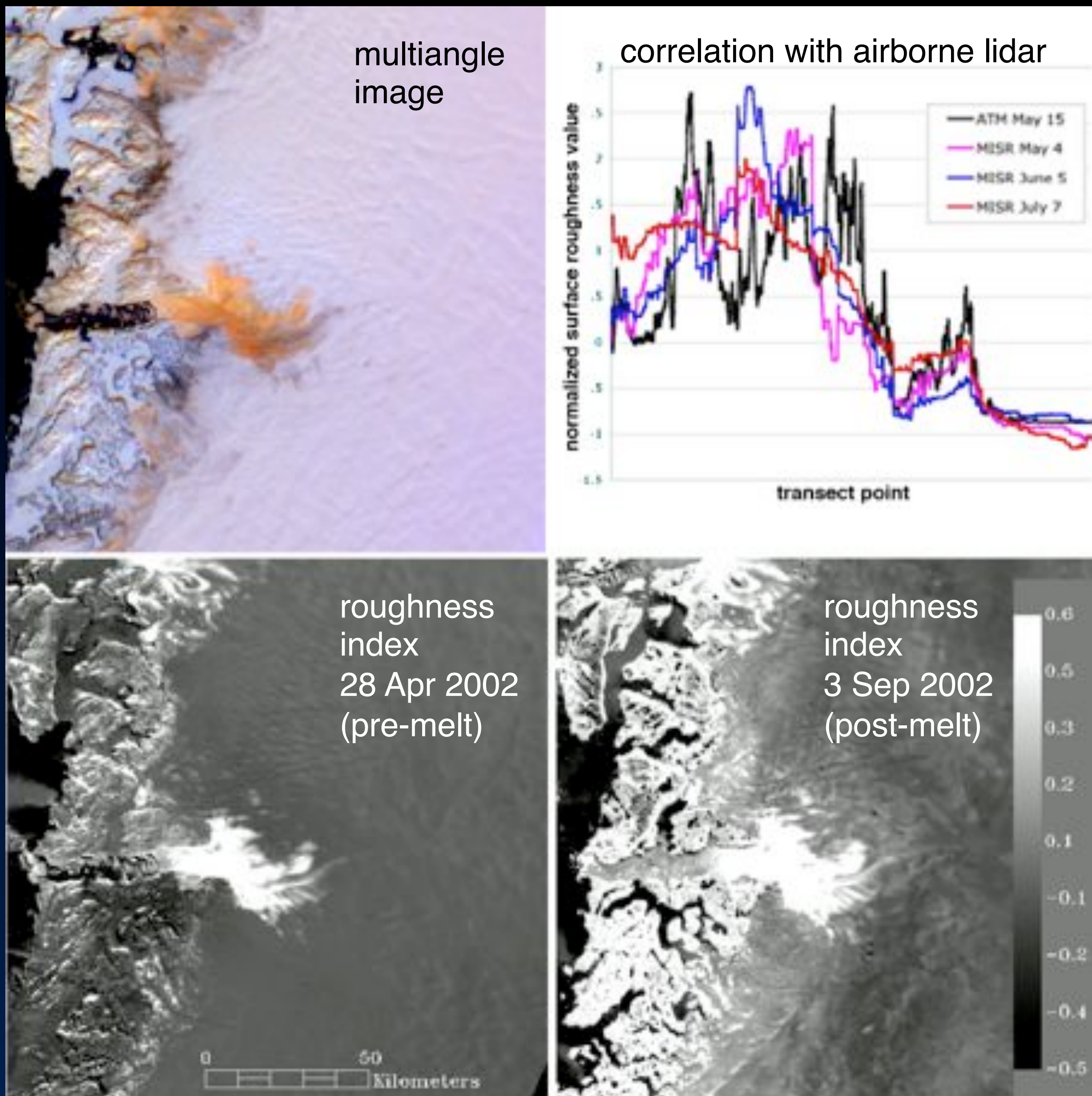

Changes in ice sheet surface roughness

Surface morphology is influenced by ice accumulation, ablation, and melt.

Spatial and temporal changes in ice sheet roughness are revealed in MISR data.

Jakobshavn glacier, Greenland

A. Nolin et al. (2002), TGARS

Distinguishing sea ice types

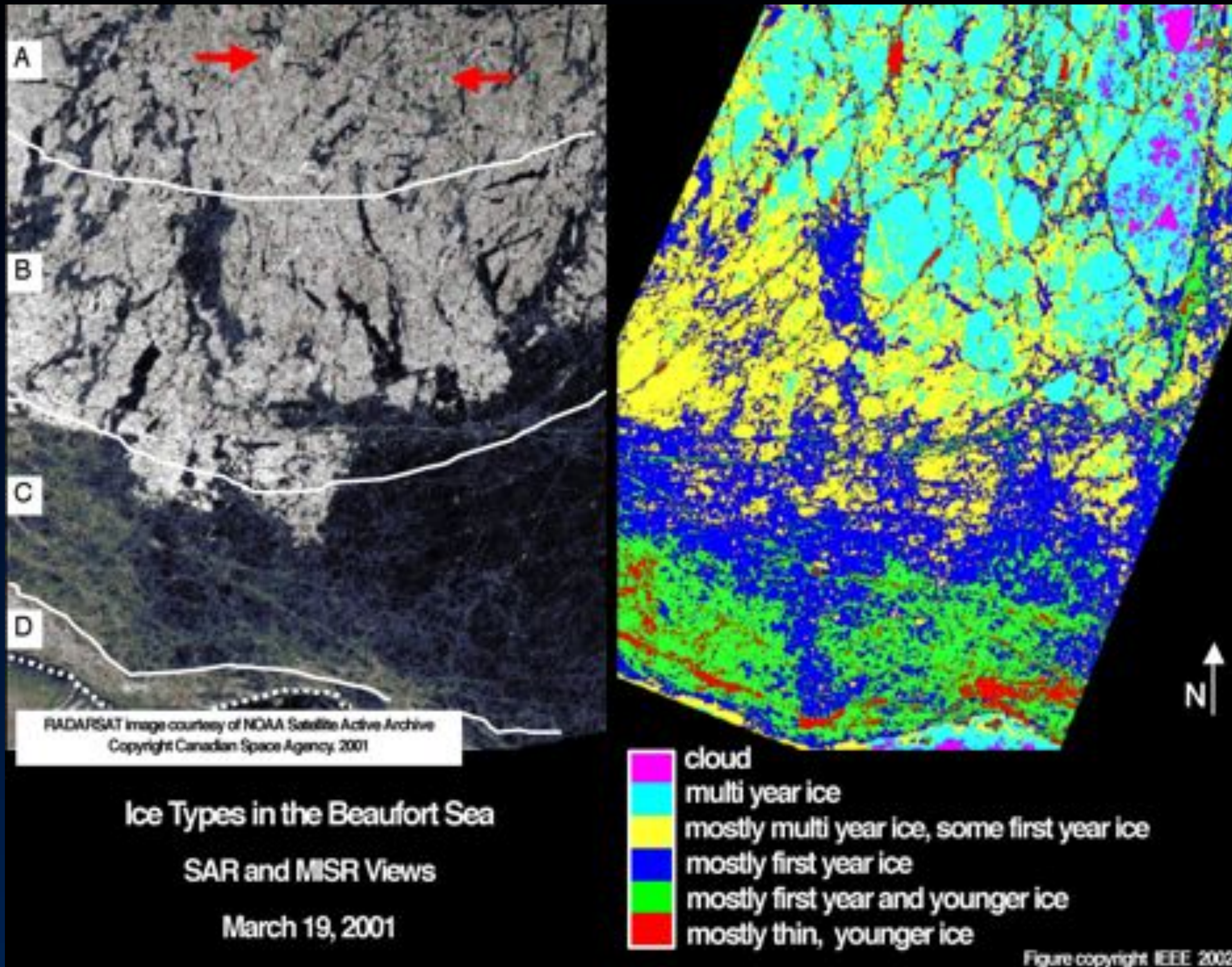

A. Nolin et al. (2002), TGARS

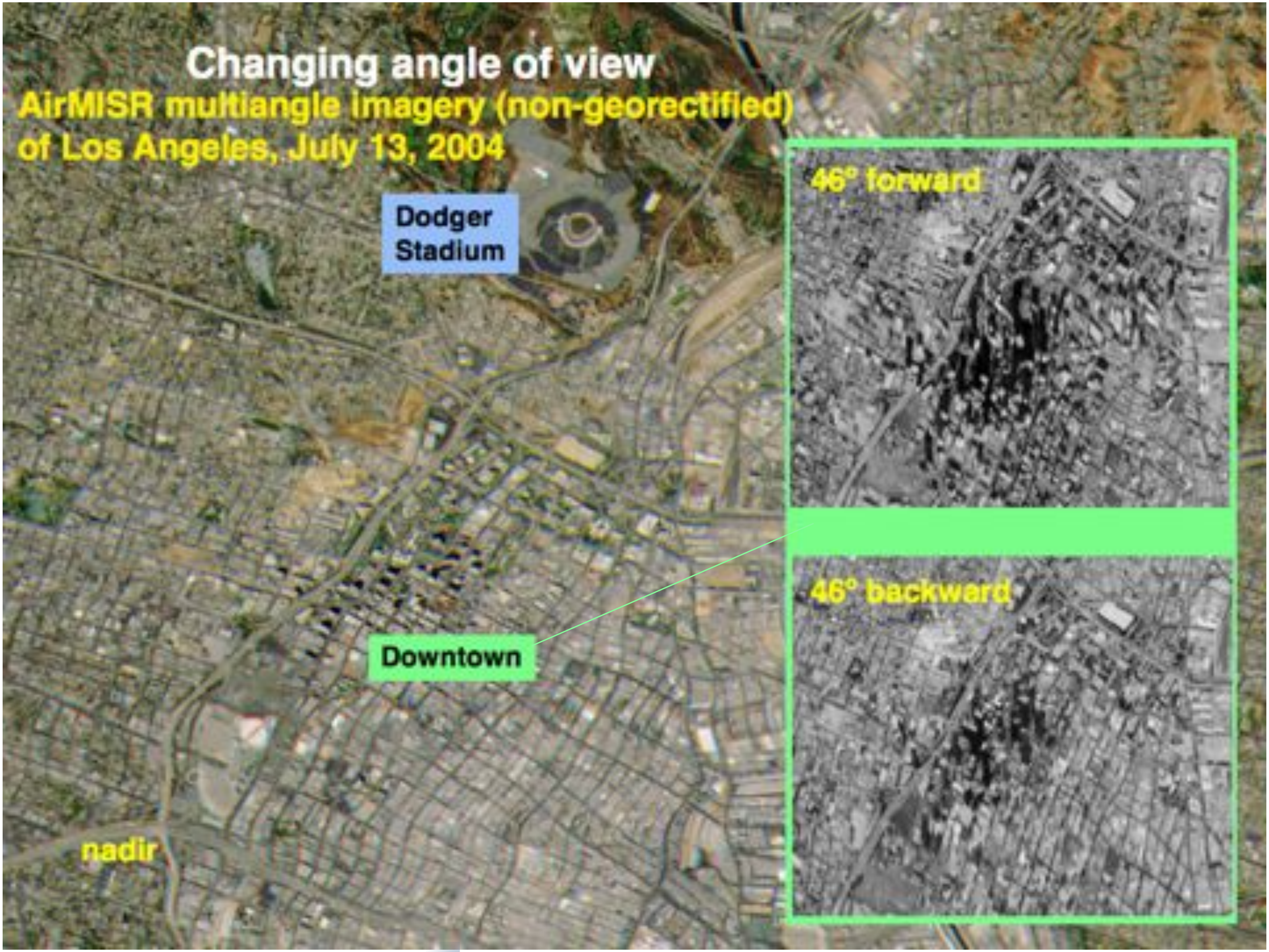

Changing angle of view
AirMISR multiangle imagery (non-georectified)
of Los Angeles, July 13, 2004
Dodger
Stadium
Downtown
nadir
46° forward
46° backward

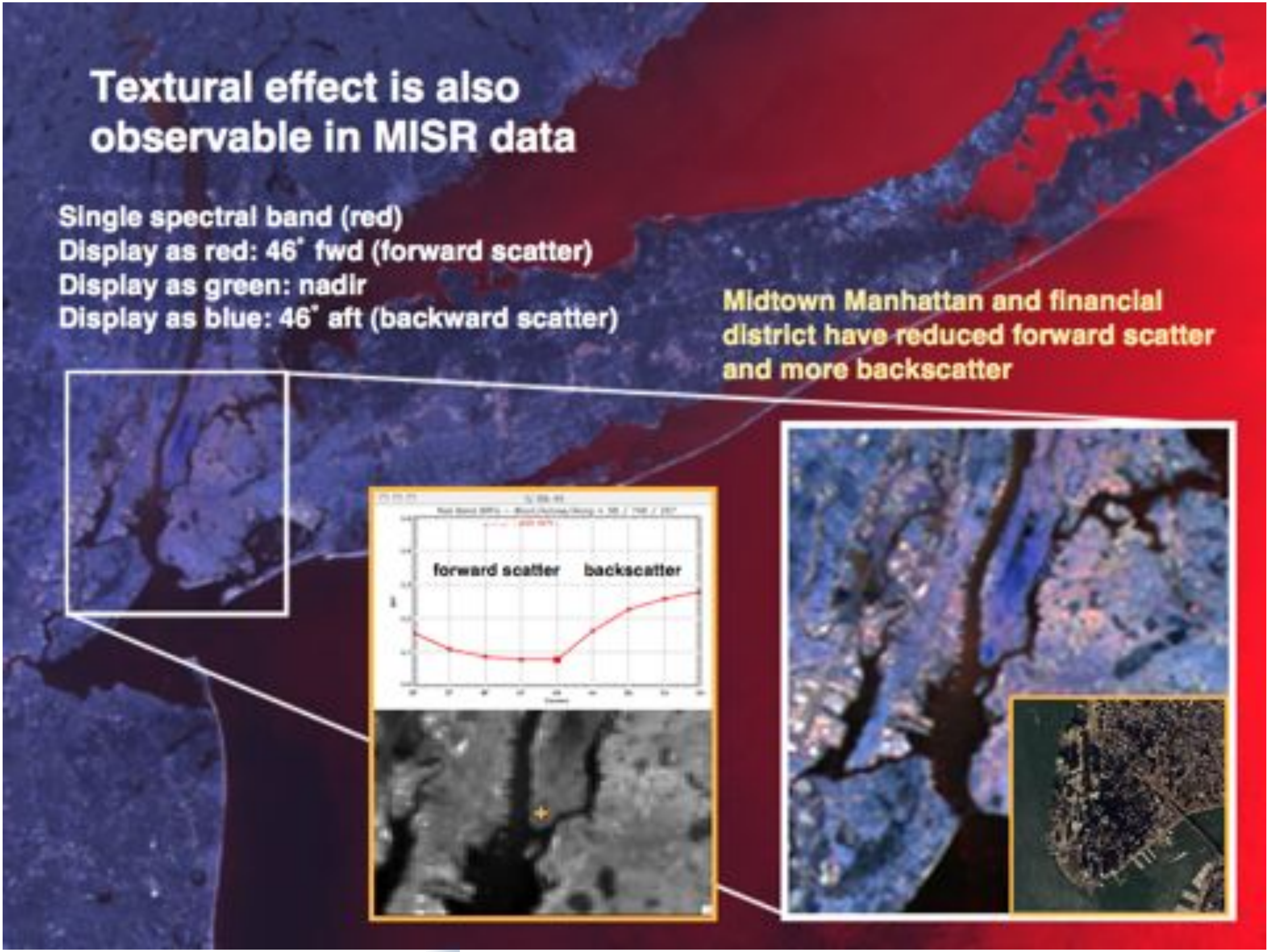
Textural effect is also observable in MISR data
Single spectral band (red)
Display as red: 46° fwd (forward scatter)
Display as green: nadir
Display as blue: 46° aft (backward scatter)
Midtown Manhattan and financial district have reduced forward scatter and more backscatter
forward scatter
backscatter


Cape Hatteras, NC
11 October 2000
26° aft red, green, blue


Cape Hatteras, NC
11 October 2000
26° forward red, green, blue

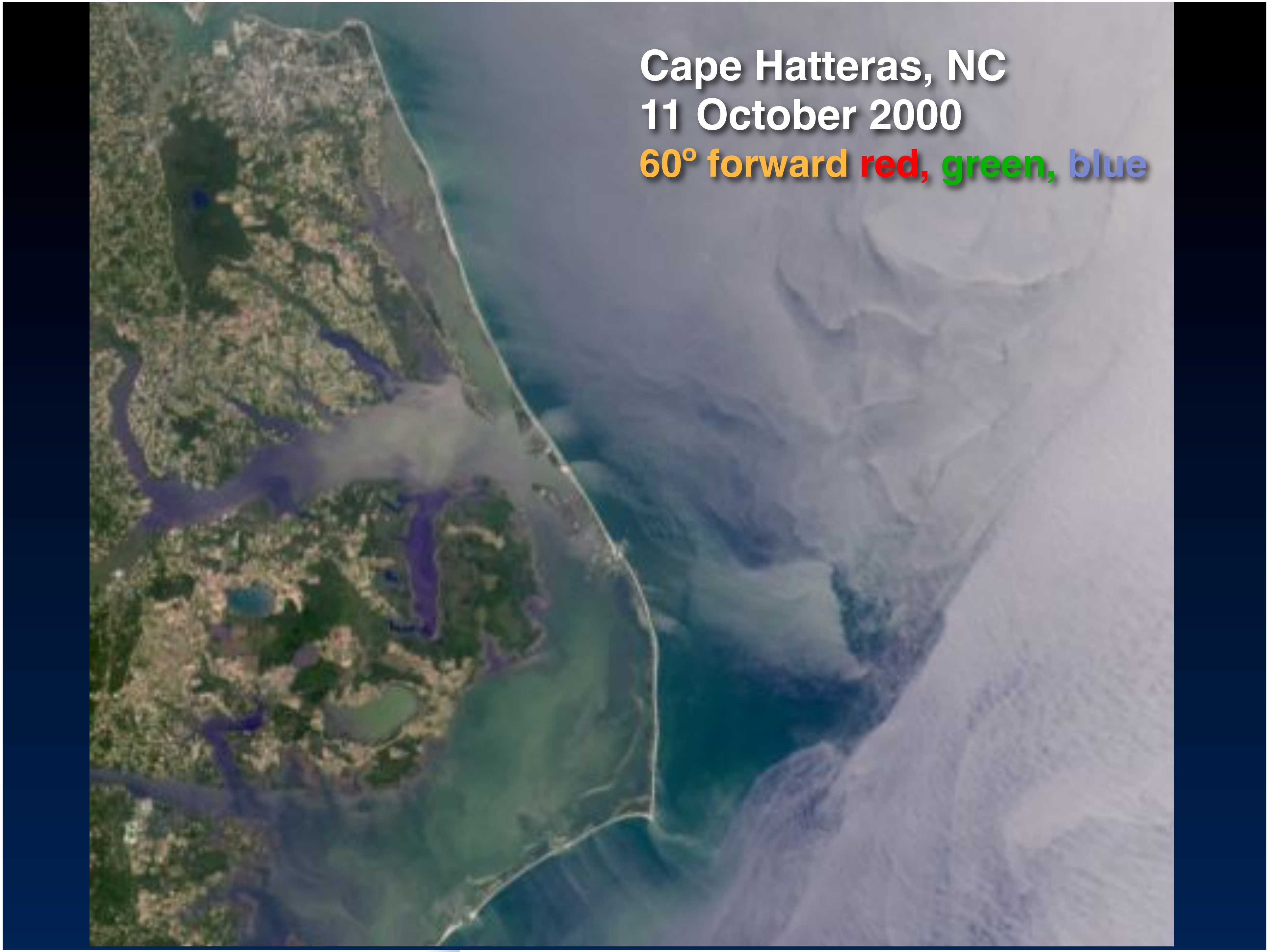
Cape Hatteras, NC
11 October 2000
60° forward red, green, blue

Sunglint as a source of information on surface wind speed

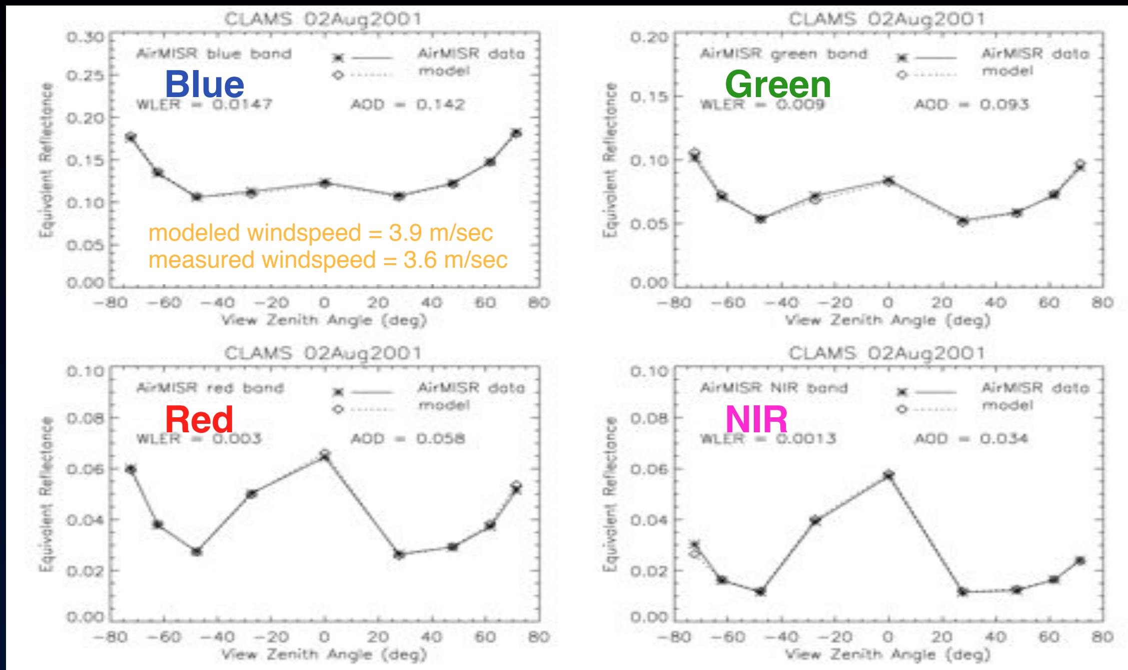

AirMISR data over the Chesapeake Lighthouse 8/2/2001

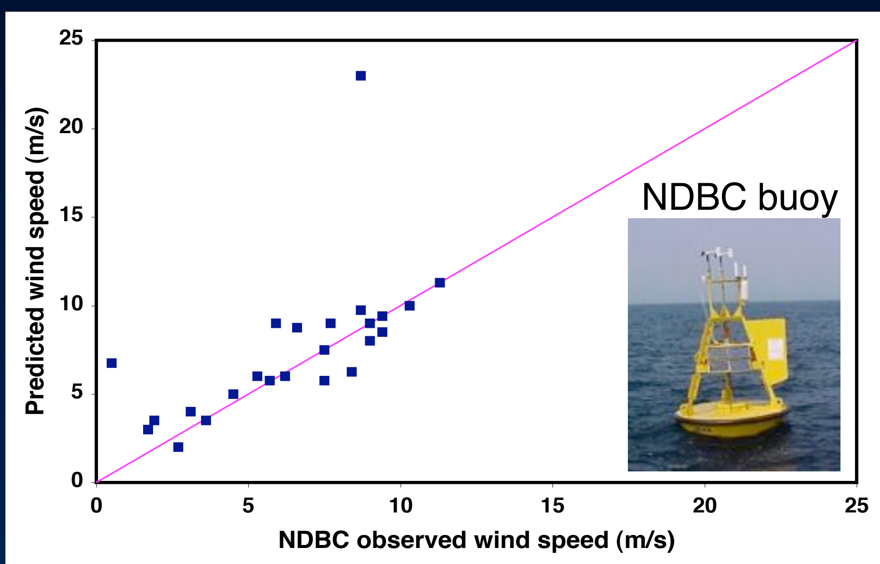

2000-2002 MISR-retrieved surface wind speed compared to NOAA National Data Buoy Center (NDBC) measurements (13 sites near California and Hawaii)

RMS error = 3 m/s (all points); 1 m/s (without outliers)

D. Fox, E. Gonzales, R. Kahn, J. Martonchik, submitted to Rem. Sens. Environ.

Bidirectional reflectance at top-of-atmosphere

San Joaquin Valley
3 January 2001

nadir

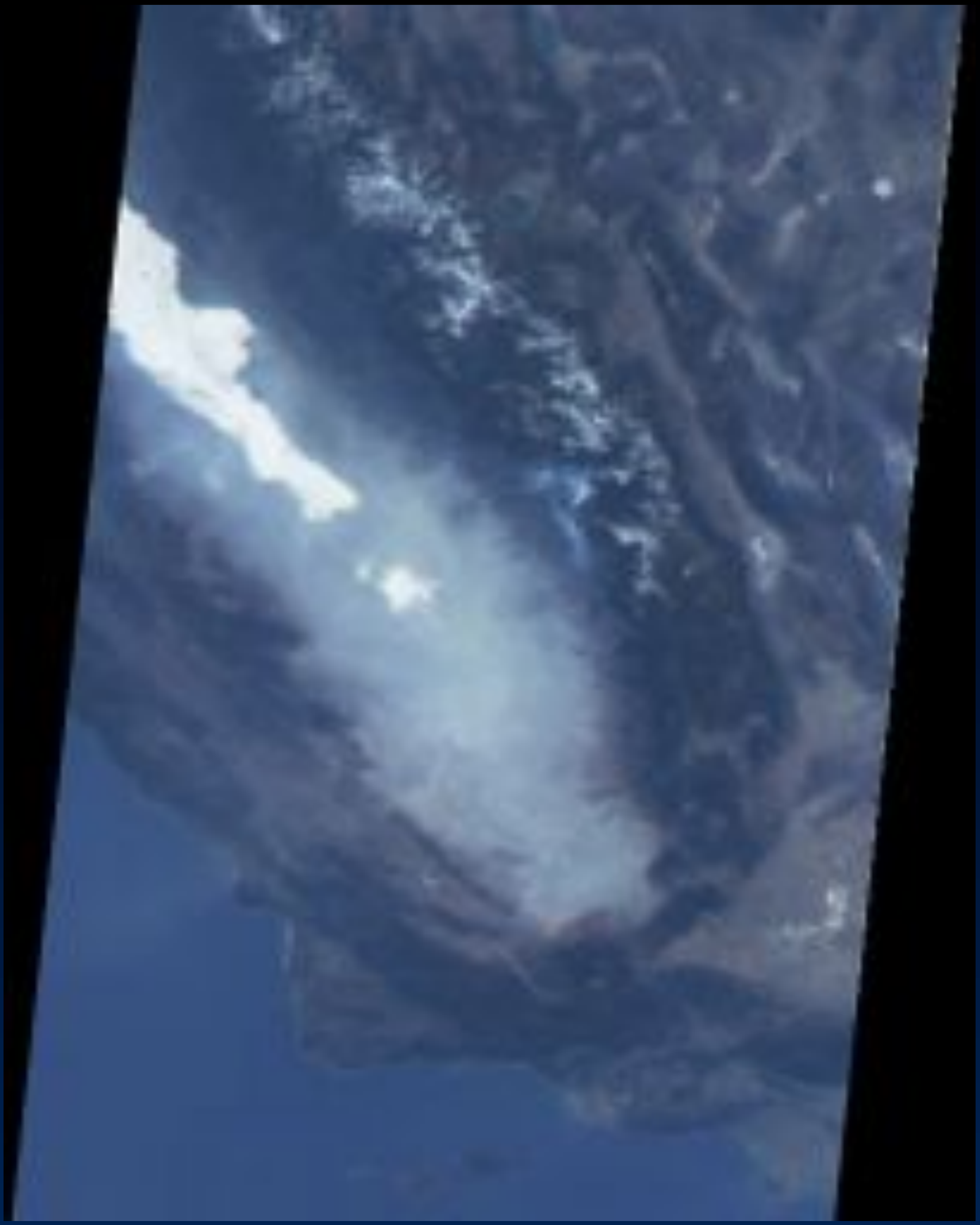

Bidirectional reflectance at top-of-atmosphere

San Joaquin Valley
3 January 2001

70º forward

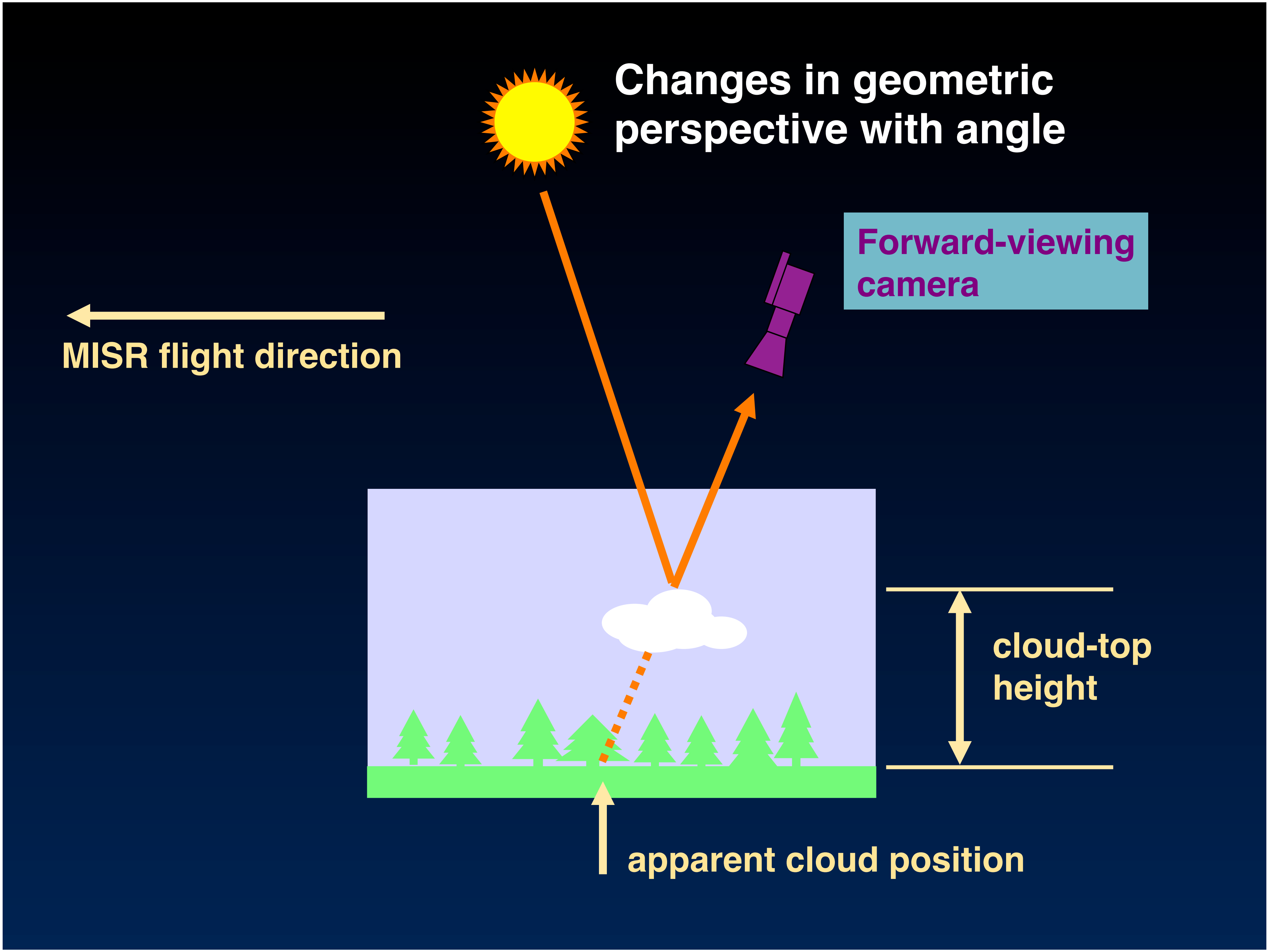
Changes in geometric perspective with angle
Forward-viewing camera
MISR flight direction
cloud-top height
apparent cloud position

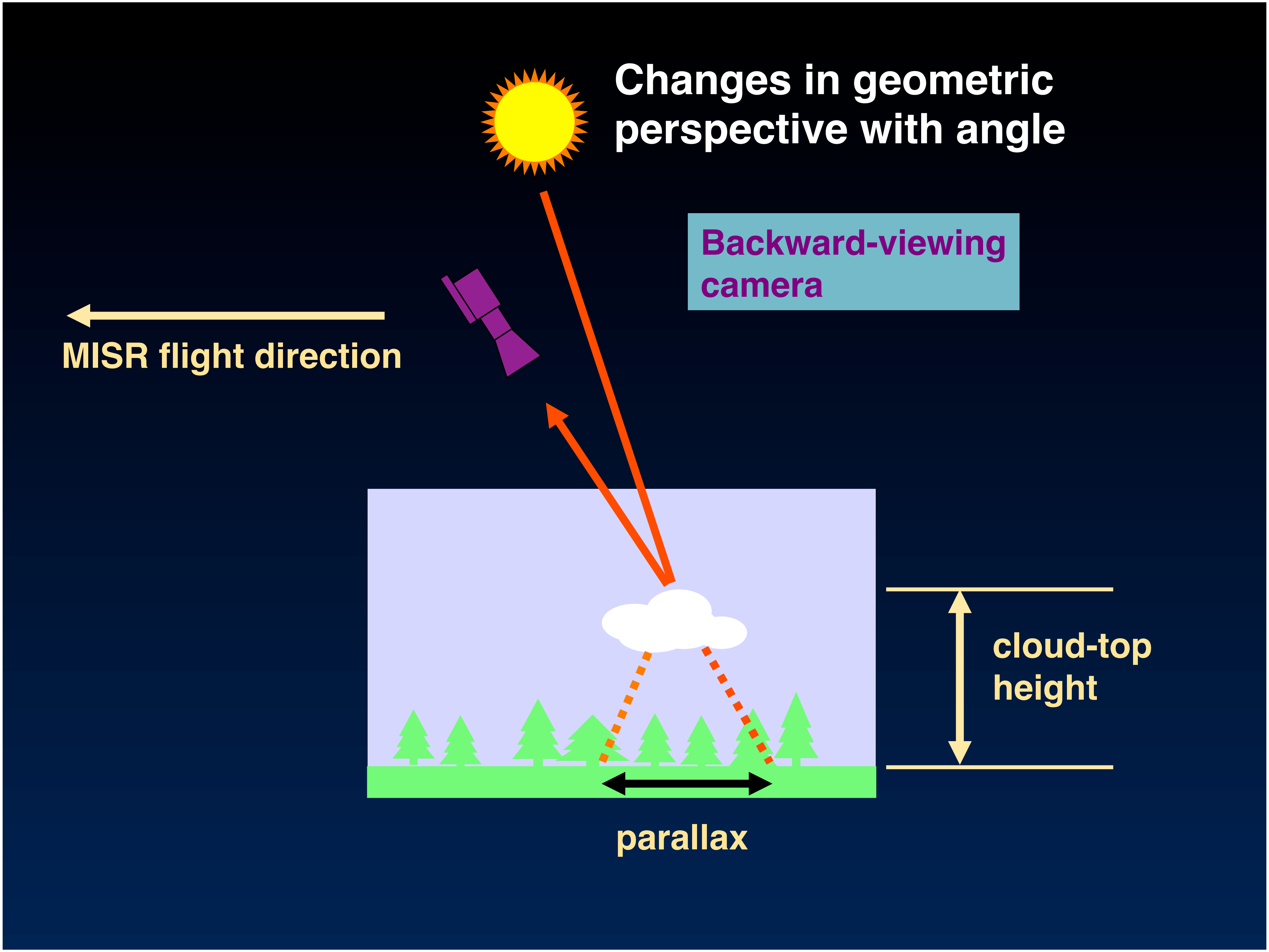
Changes in geometric perspective with angle
Backward-viewing camera
MISR flight direction
cloud-top height
parallax

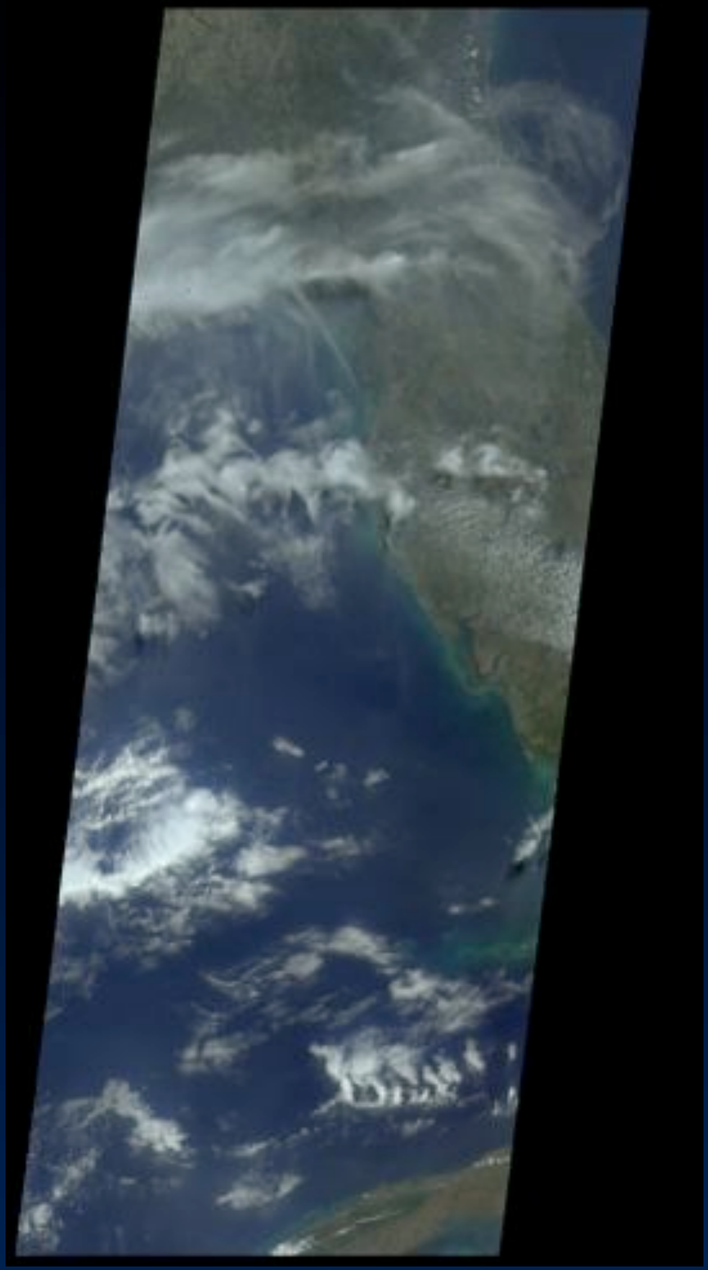

Multiangle "flyover"
Florida and Cuba
6 March 2000

Georgian Bay, Ontario, 6 March 2000

Nadir (An)

70° forward (Df)

Georgian Bay, Ontario, 6 March 2000

Nadir (An)

60° forward (Cf)

Georgian Bay, Ontario, 6 March 2000

Nadir (An)

46° forward (Bf)

Georgian Bay, Ontario, 6 March 2000

Nadir (An)

26º forward (Af)

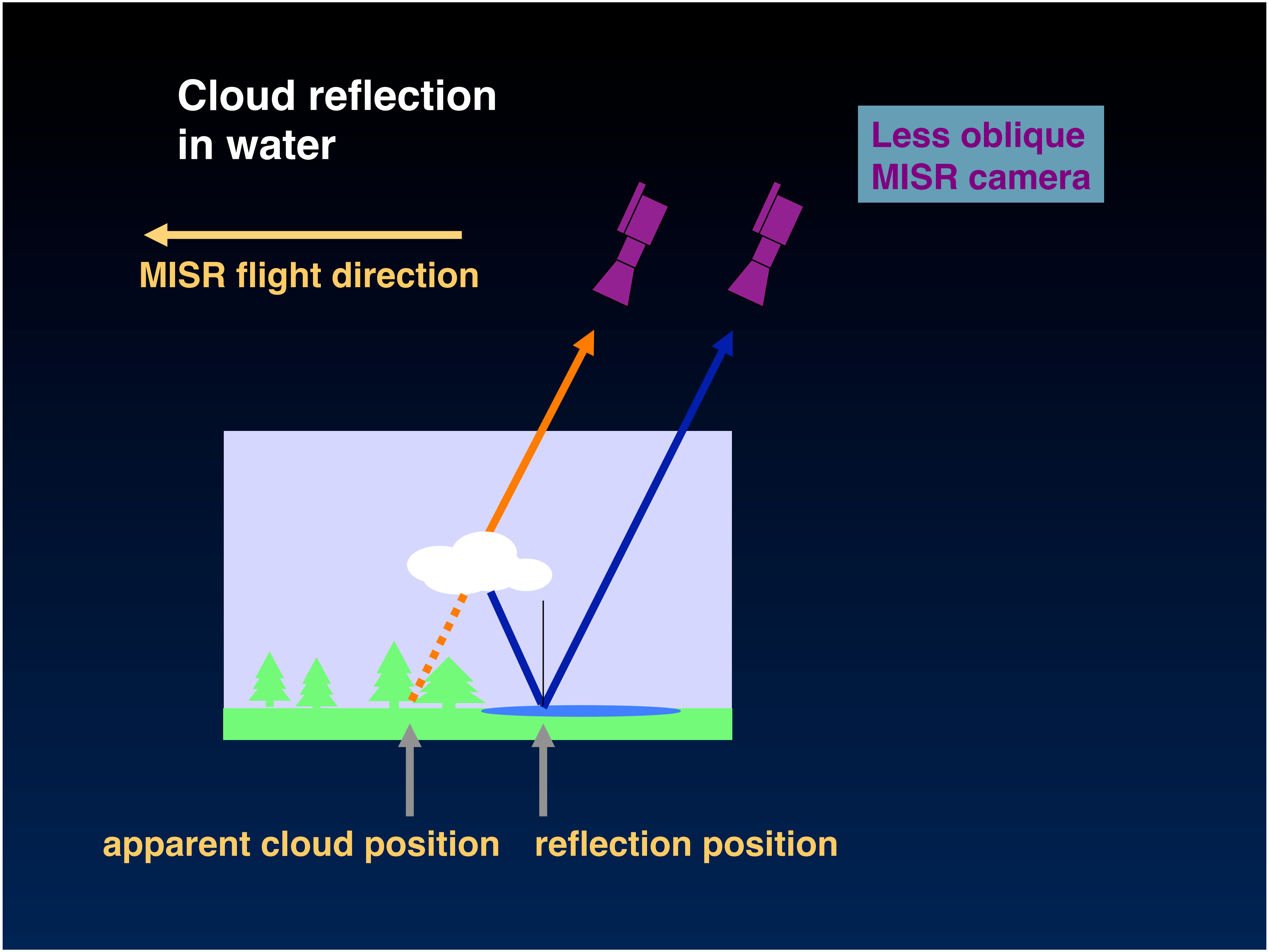
Cloud reflection
in water
Less oblique
MISR camera
MISR flight direction
apparent cloud position
reflection position

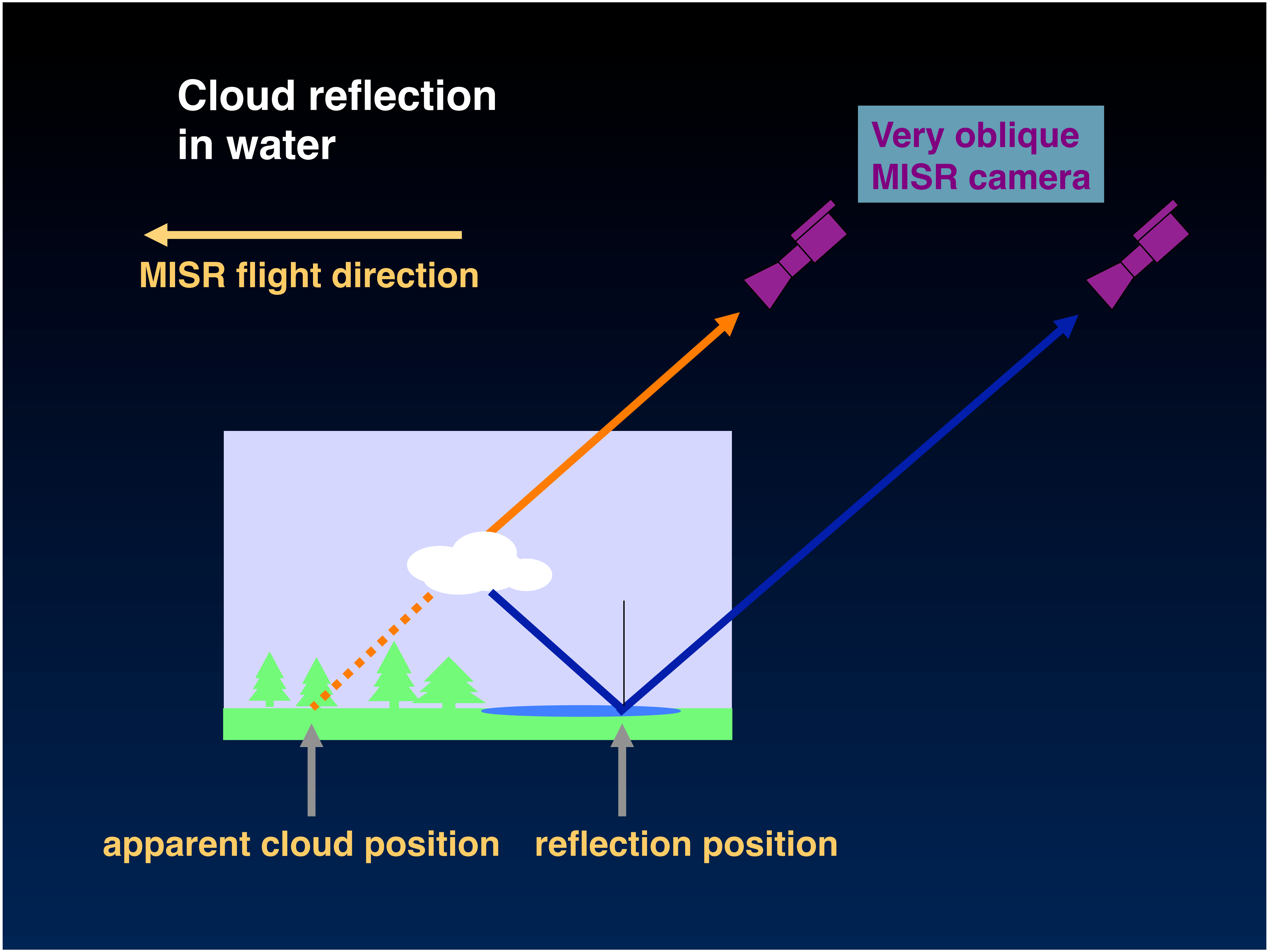
Cloud reflection
in water
Very oblique
MISR camera
MISR flight direction
apparent cloud position
reflection position

Himalayas

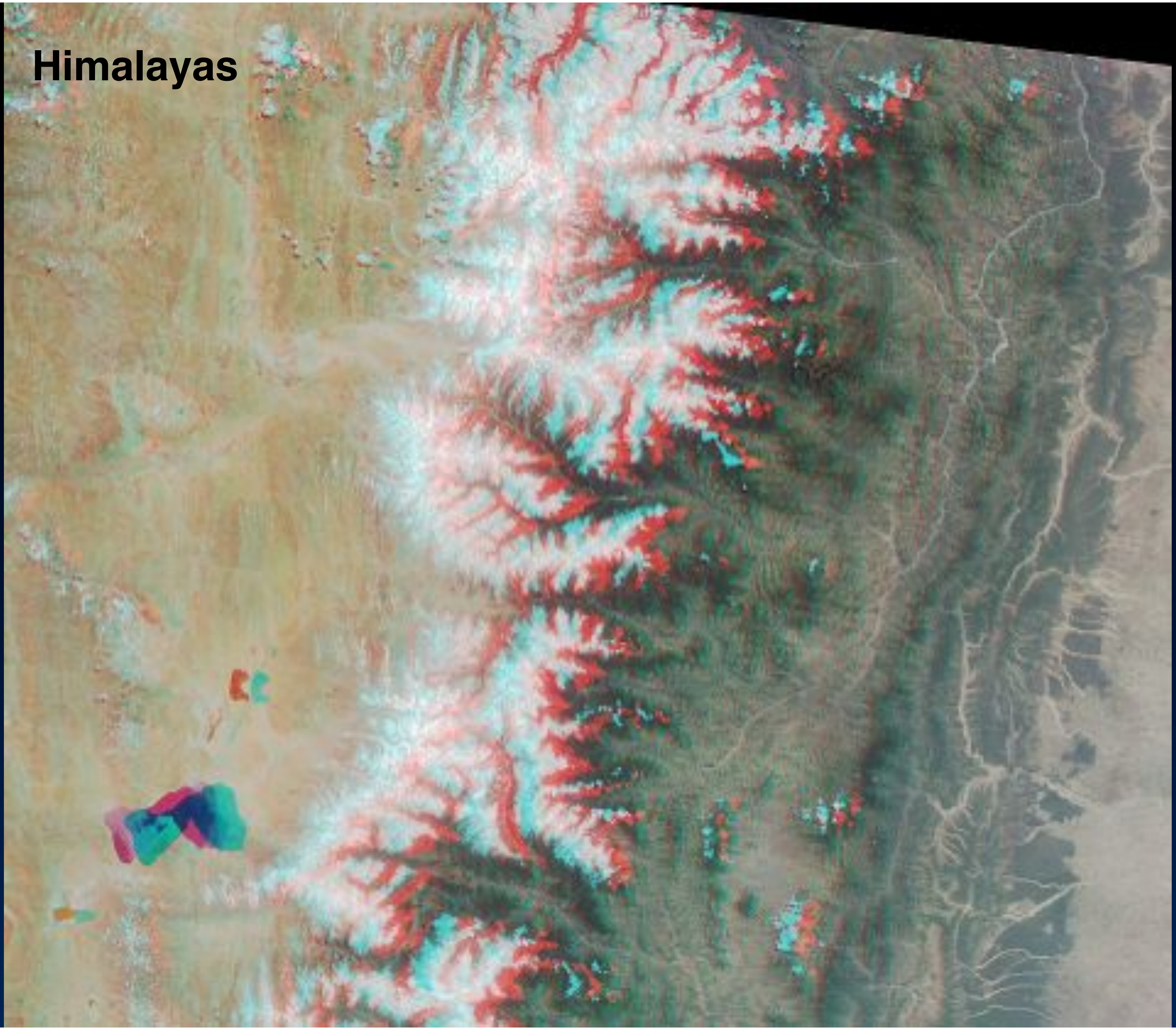

Eruption of Mt. Etna, 22 July 2001

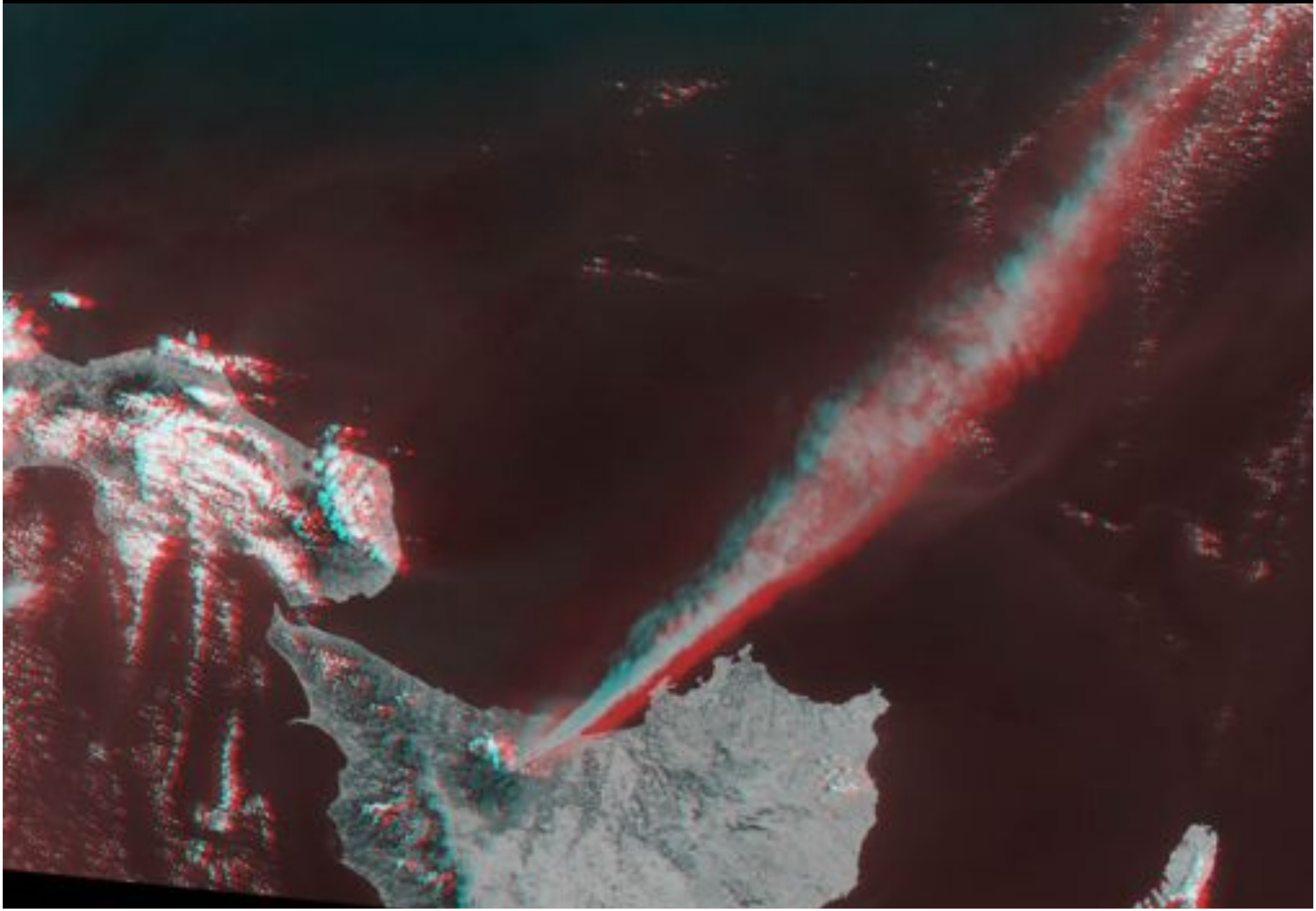

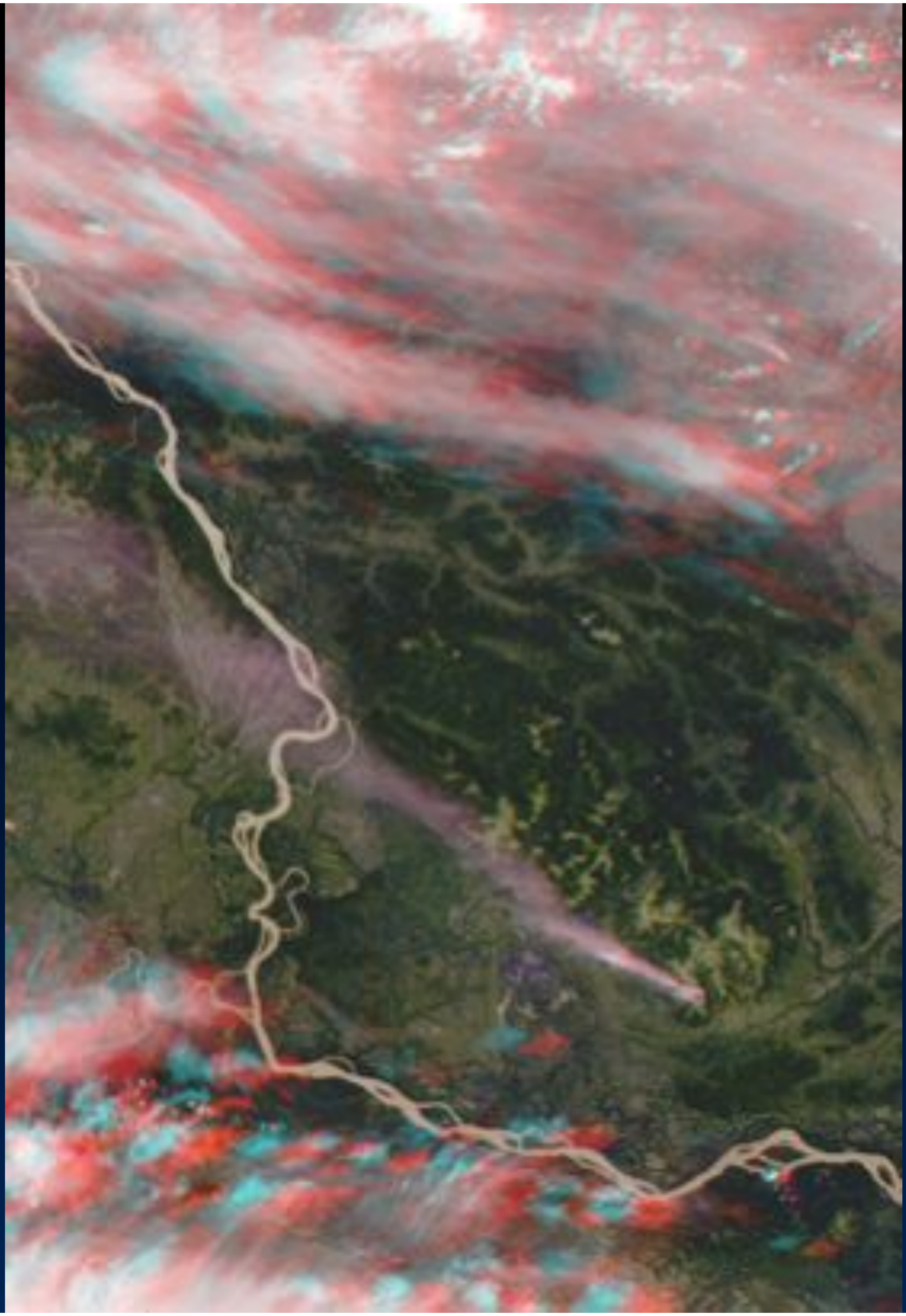

Alaskan
Wildfire
and
Cirrus Clouds

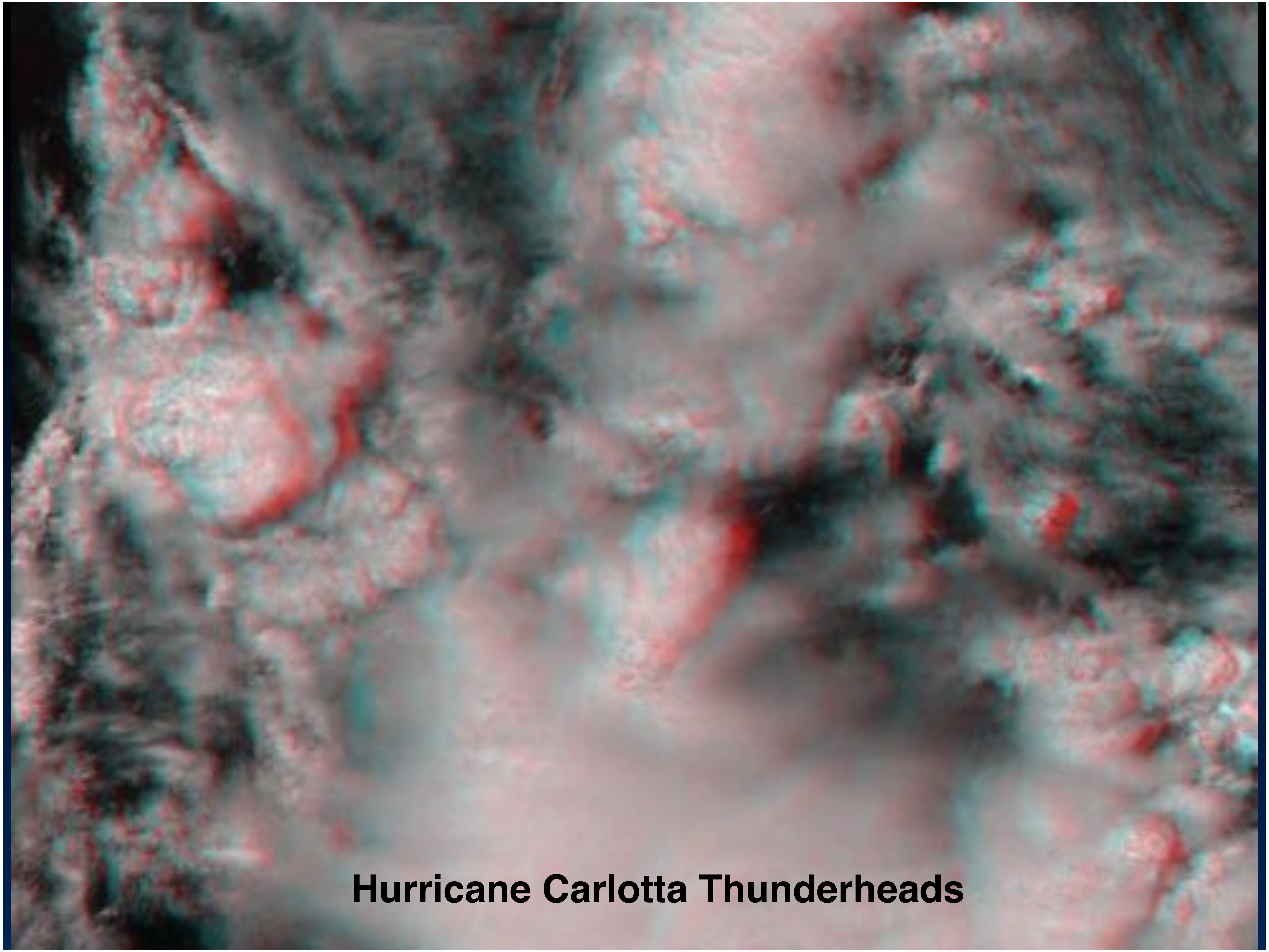

Hurricane Carlotta Thunderheads

Hurricane Alberto Eye

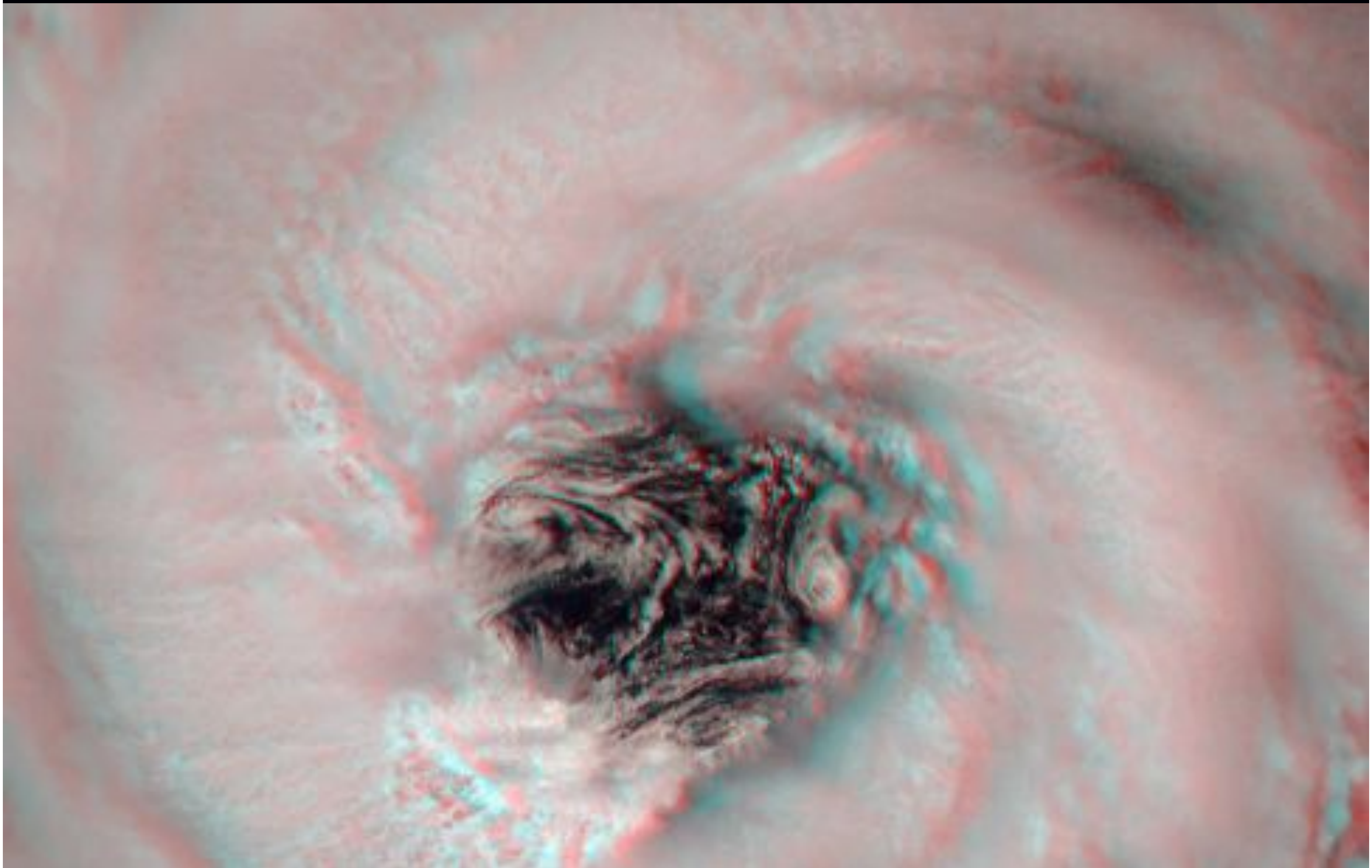

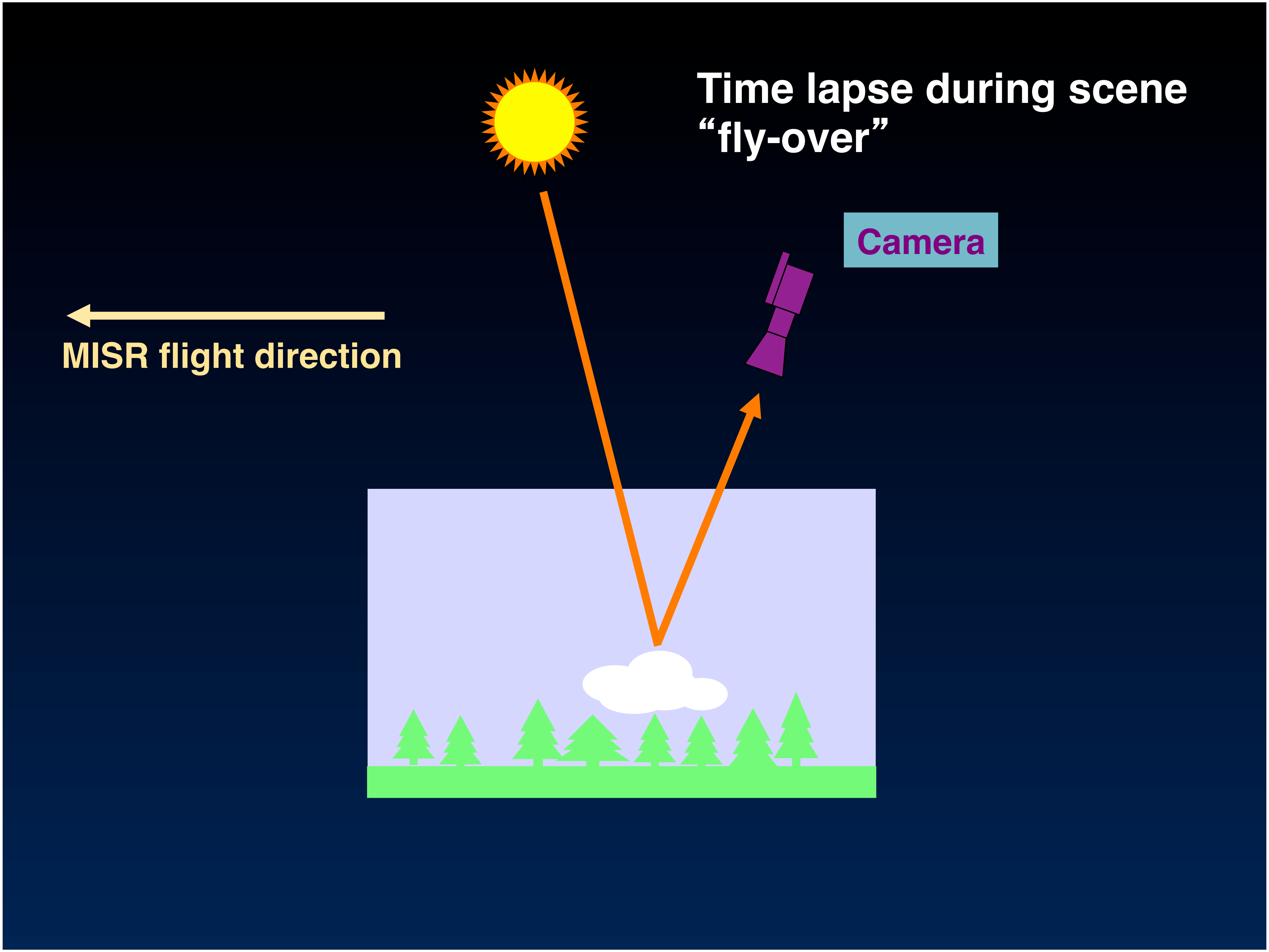
Time lapse during scene
“fly-over”
Camera
MISR flight direction

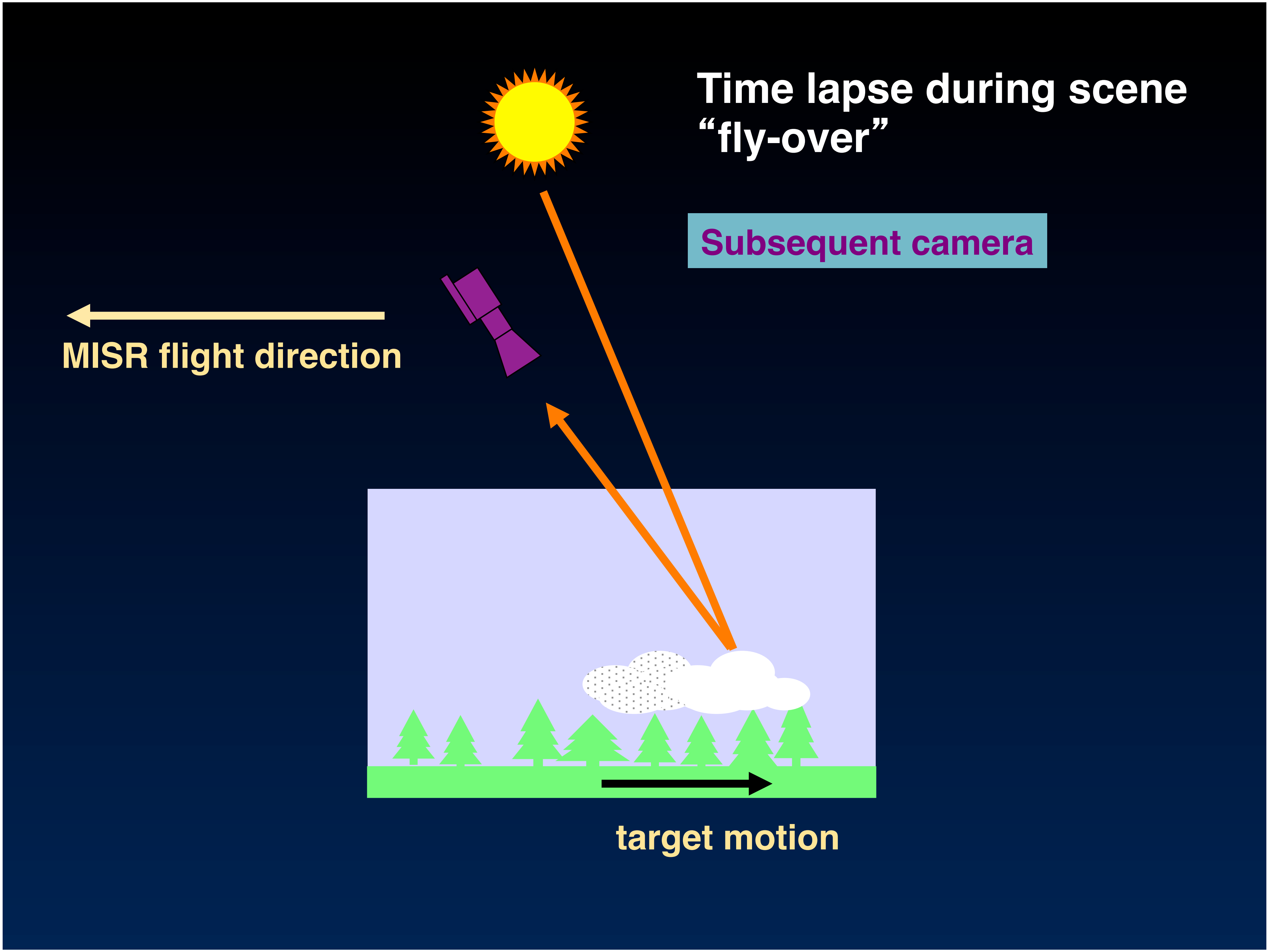
Time lapse during scene
“fly-over”
Subsequent camera
MISR flight direction
target motion

Moving ships off the North Carolina Coast

11 October 2000

Von Karman vortex street near Jan Mayen Island

6 June 2001


Indian coast
Godavari River Delta
Approx. 16.4ºN, 81.8ºE
26 December 2004
86 km
49 km
MISR 60º fwd - 70º aft
05:11 - 05:17 UTC
cloud motion is due to parallax
resulting from their height above the surface;
tsunami waves are at sea level and
show actual motion
10 km

L1B2 Geometric Parameters

Provided on 17.6-km centers

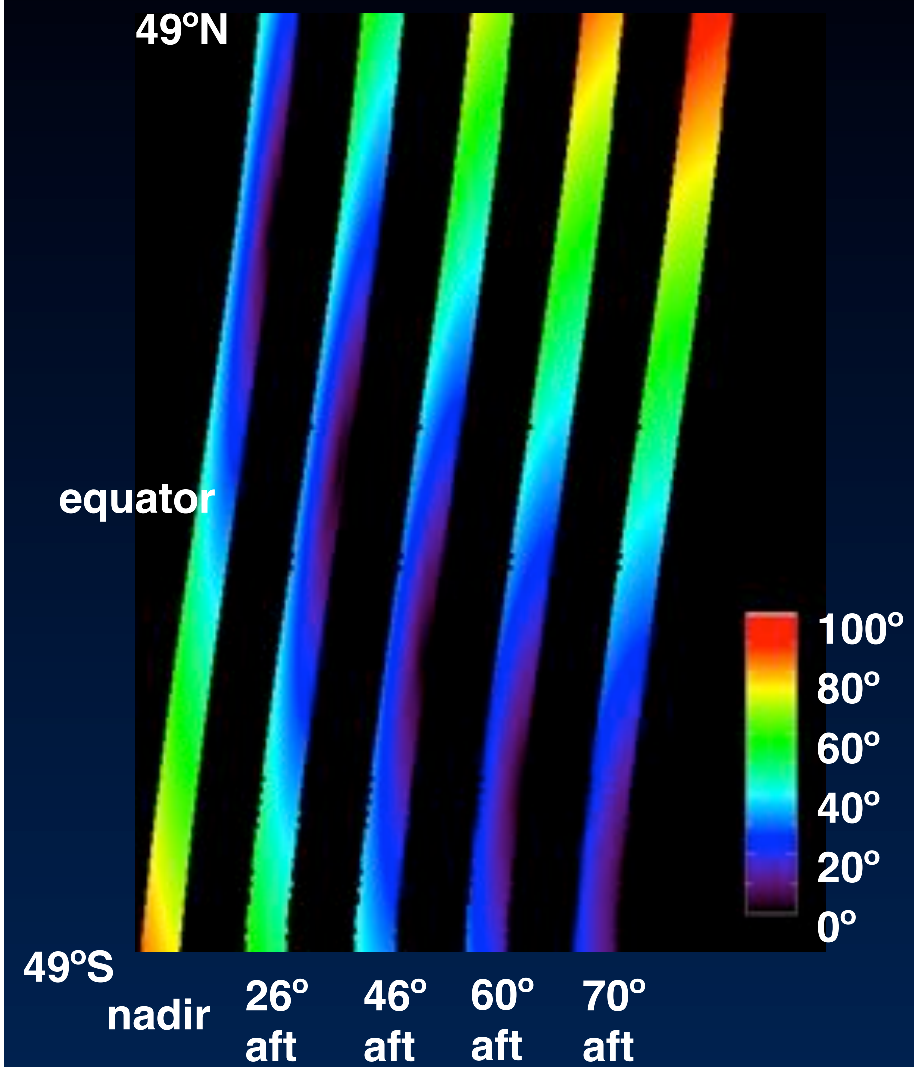

Example of glitter angle July 3

CONTENTS

- View zenith and azimuth angles per camera; azimuths measured relative to local north
- Solar zenith and azimuth angles correspond to midpoint viewing time of only those cameras which observed the point
- Scatter and glitter angles also included in product

Level 2 Standard Products

Level 2 standard products

- Level 2TC stereo
- Level 2TC cloud classifiers
- Level 2TC top-of-atmosphere albedo
- Level 2AS aerosol
- Level 2AS land surface

Level 2 processing uses multiple cameras simultaneously

- Angular radiance signatures
- Geometric parallax
- Time lapse

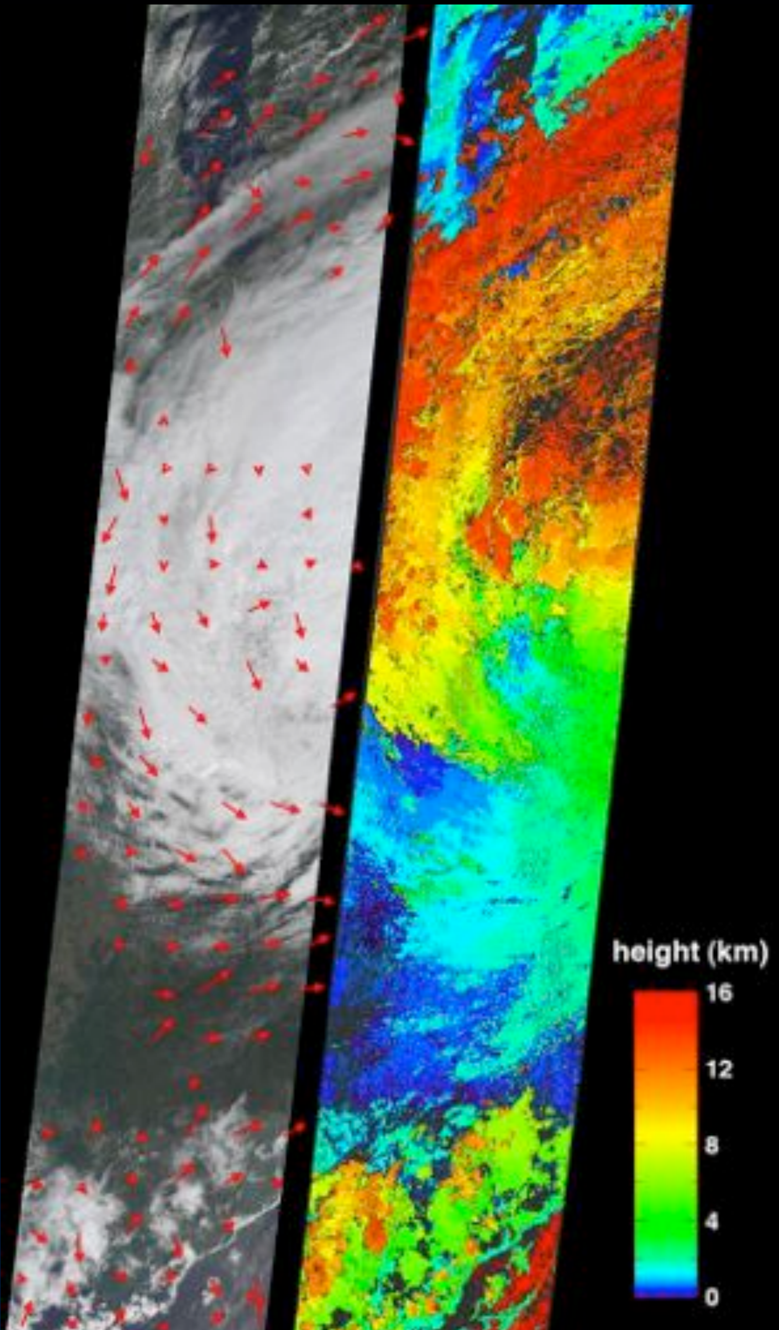

L2 TOA/Cloud Stereo Product

Cloud heights and cloud-tracked winds

HEIGHT ATTRIBUTES

- 1.1-km resolution
- Purely geometric retrievals of height
- Independent of temperature profiles and cloud emissivity
- Independent of radiometric calibration
- Accuracy 500 -1000 m

WIND ATTRIBUTES

- 70.4-km resolution
- Uses stereo triplets
- Accuracy 1-3 m/s with 300 m height resolution

Hurricane Katrina
30 August 2005

Tropical Cyclone Monty in Western Australia

29 February and 2 March 2004

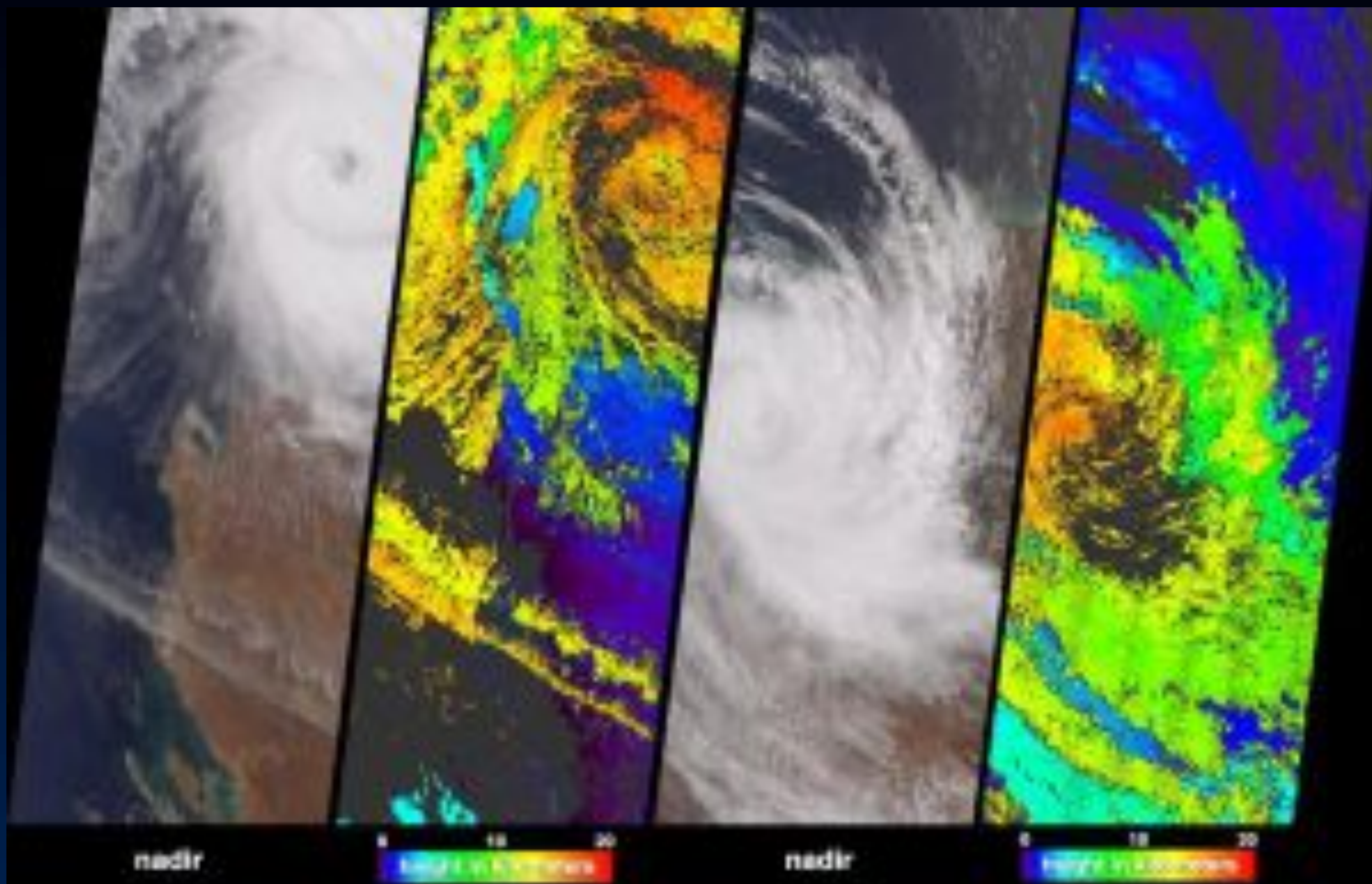

Measuring wildfire smoke plume injection and transport heights

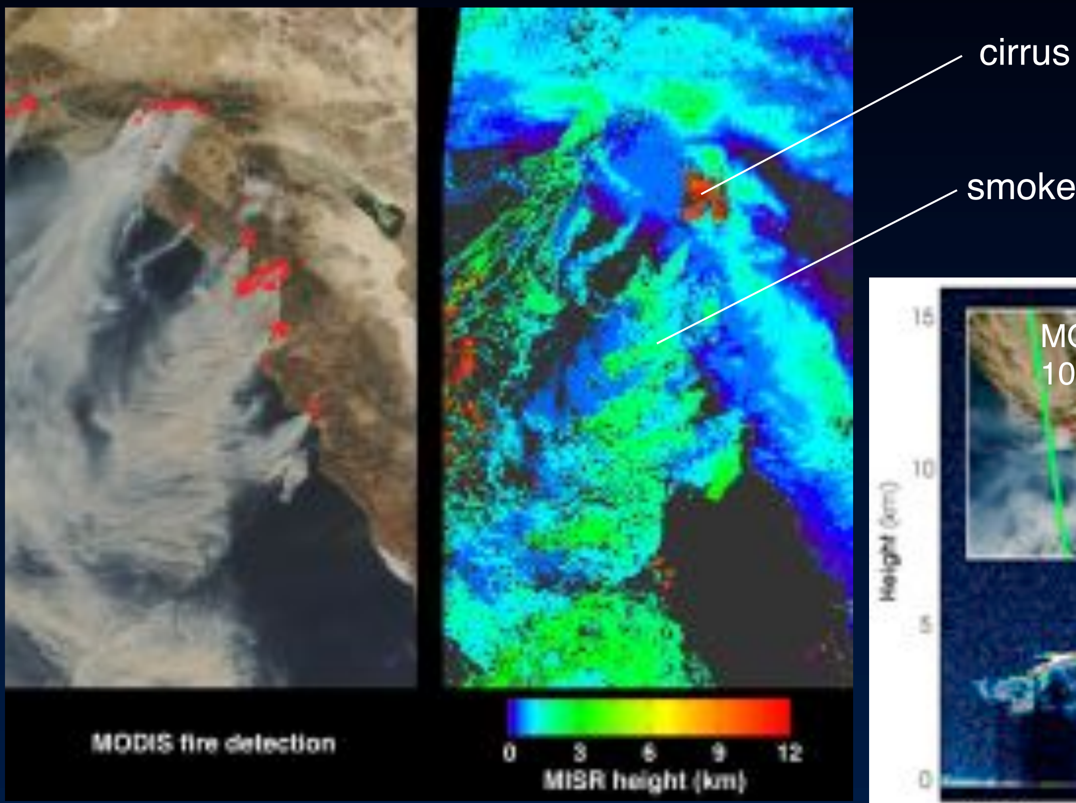

MODIS/MISR data from Terra
26 October 2003

GLAS vertical profiles
28 October 2003

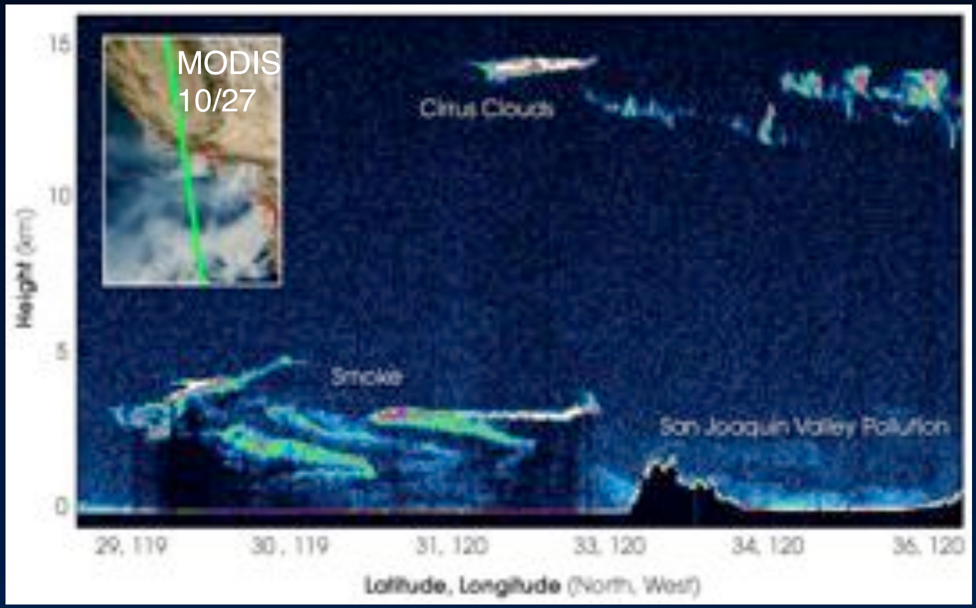

Detection of Polar Stratospheric Clouds

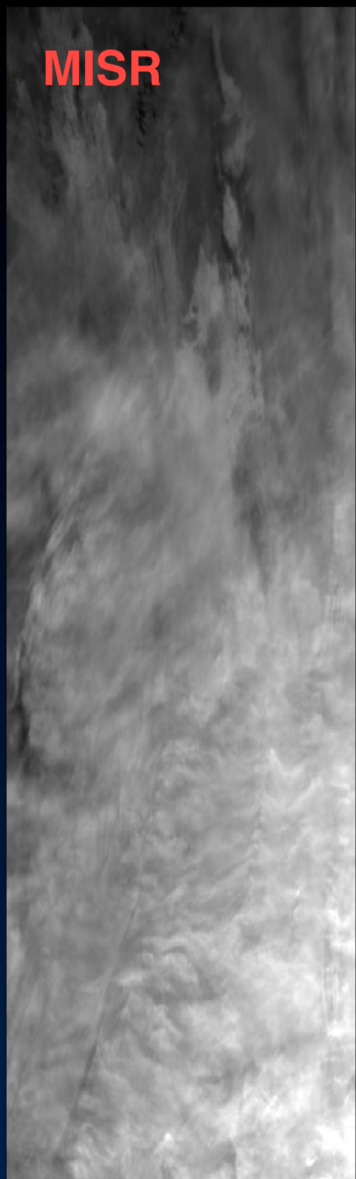

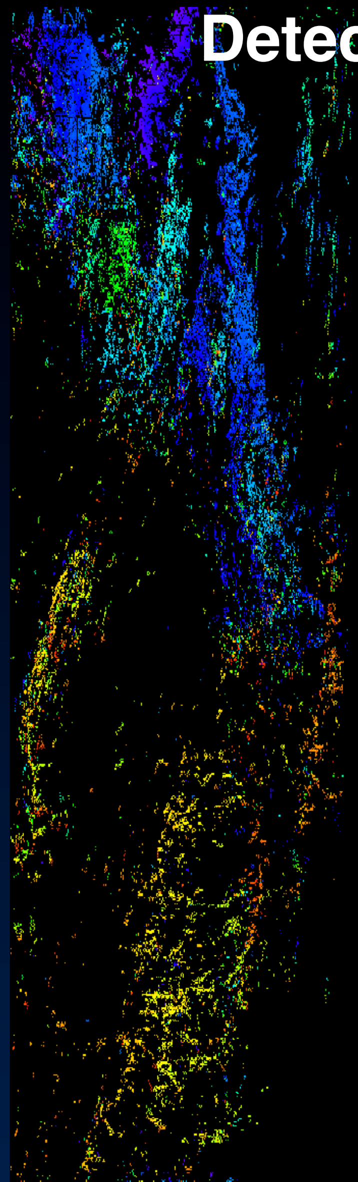

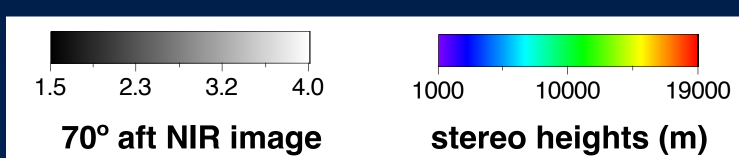

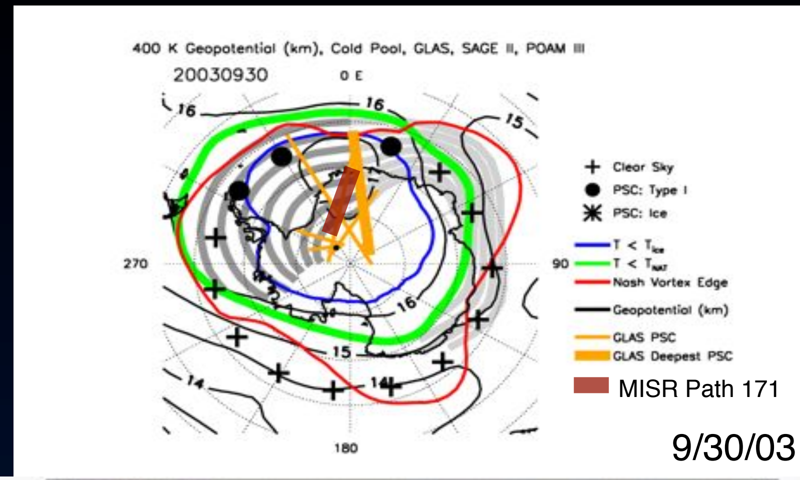

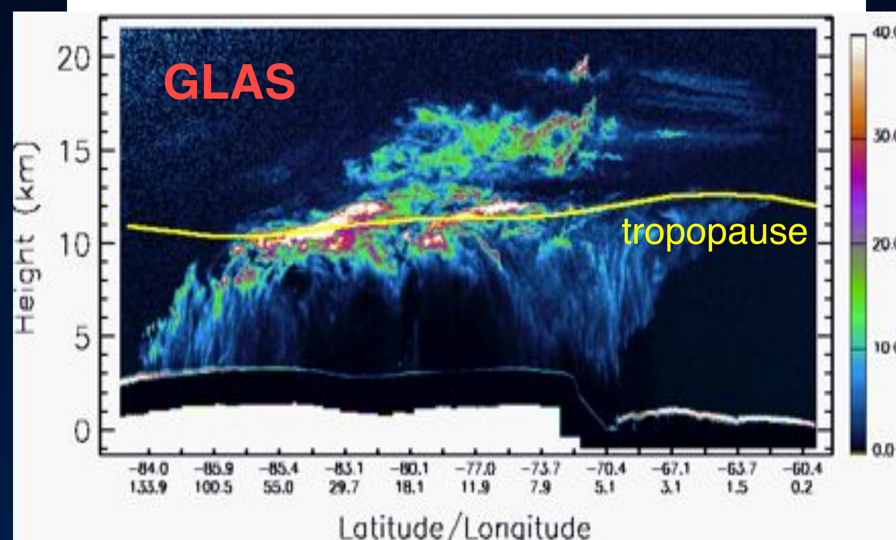

Mode and standard deviation of PSC height distributions (14 - 20 km) show **MISR-GLAS agreement to within 1 km.**

L. Di Girolamo, M. Fromm, S. Palm

L2 TOA/Cloud Albedo Product

Cloud-top-projected TOA albedo and bidirectional reflectance

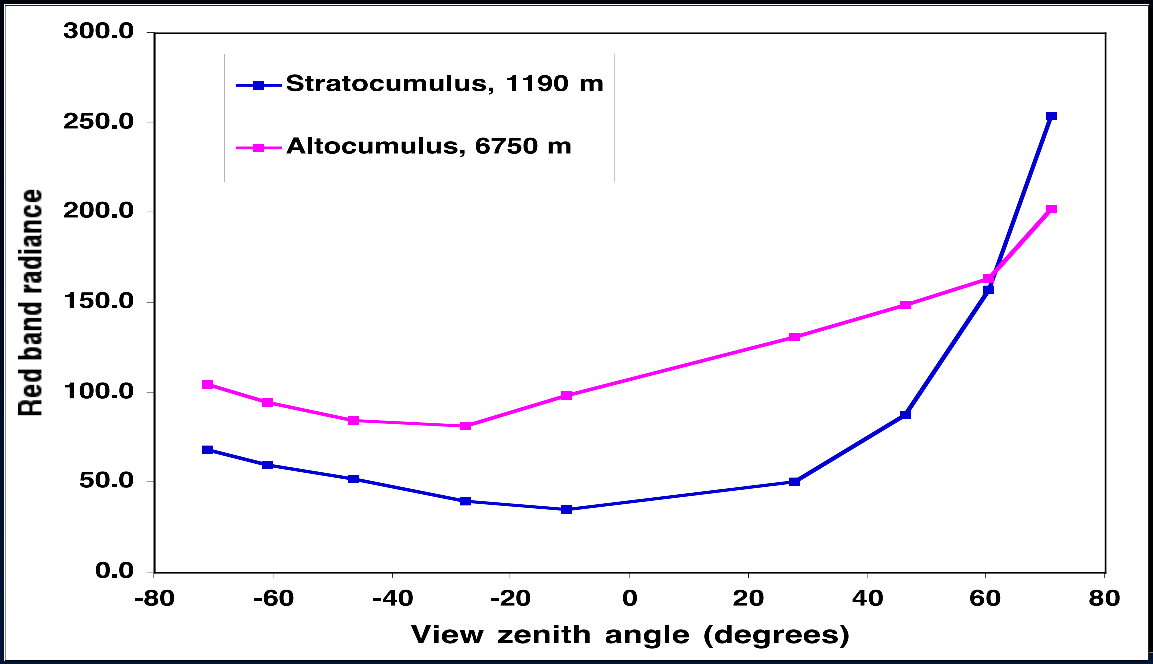

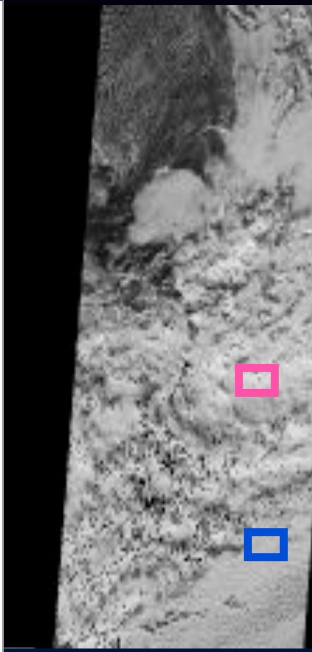

Southern Pacific Ocean, June 11, 2000

CONTENTS

- “Feature-referenced” top-of-atmosphere bidirectional reflectances
- Includes TOA albedos at fine (2.2. km) resolution for scene classification, and coarse (35.2 km resolution) for mesoscale radiation budget

Multiangle tests of cloud homogeneity

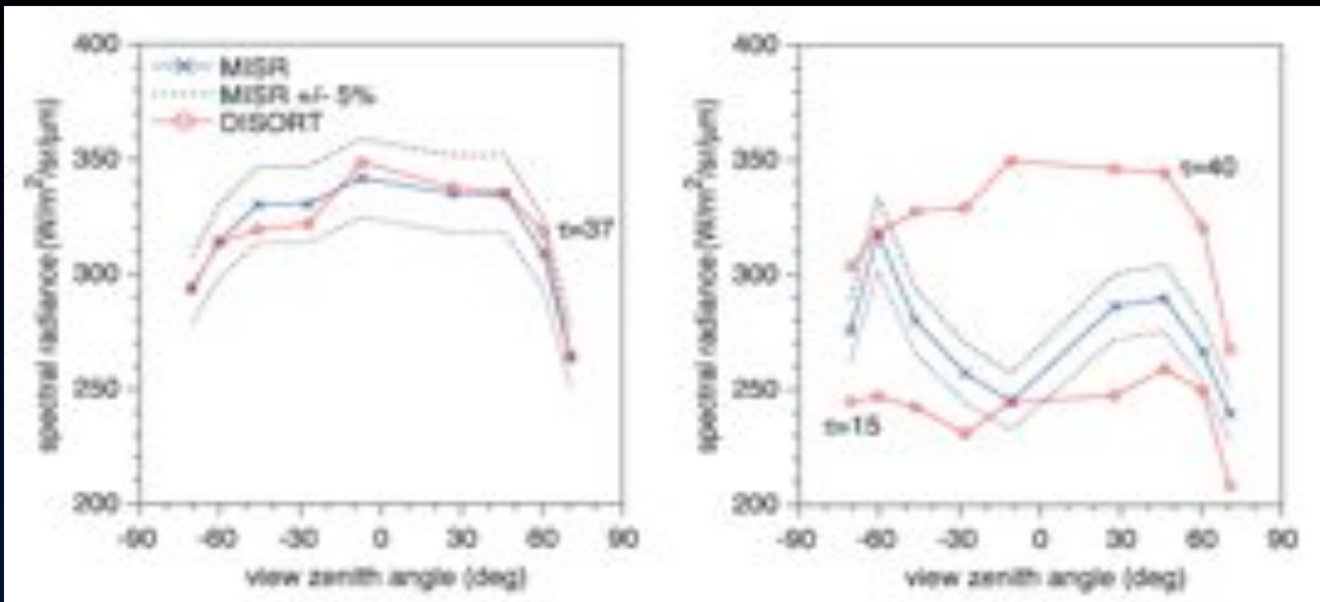

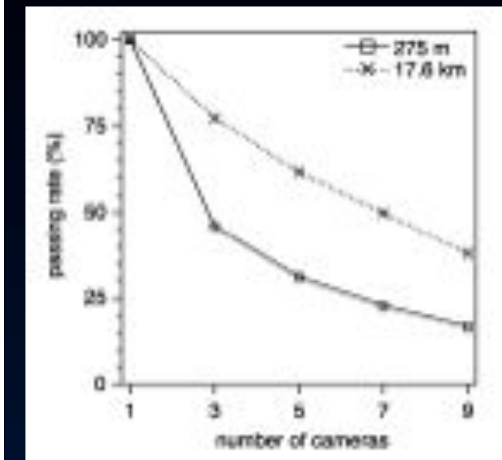

1-D theory fits MISR observations

1-D theory does not fit MISR observations

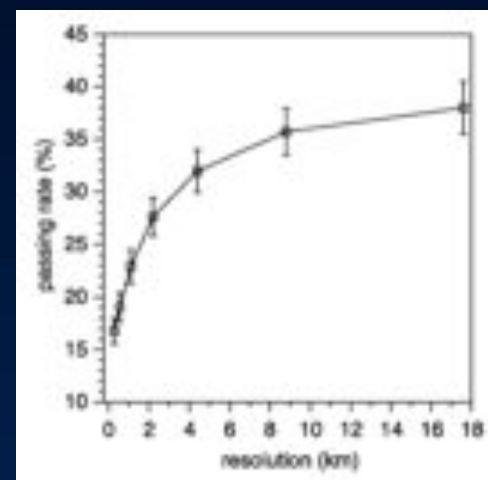

Multiangle data provides a physical consistency check on MODIS 1-D cloud retrieval assumption

Cloud morphology, not just cloud microphysics, plays a major role in determining TOA bidirectional reflectance

A. Horvath, R. Davies (2004), GRL

L2 Aerosol/Surface Product

Aerosol parameters

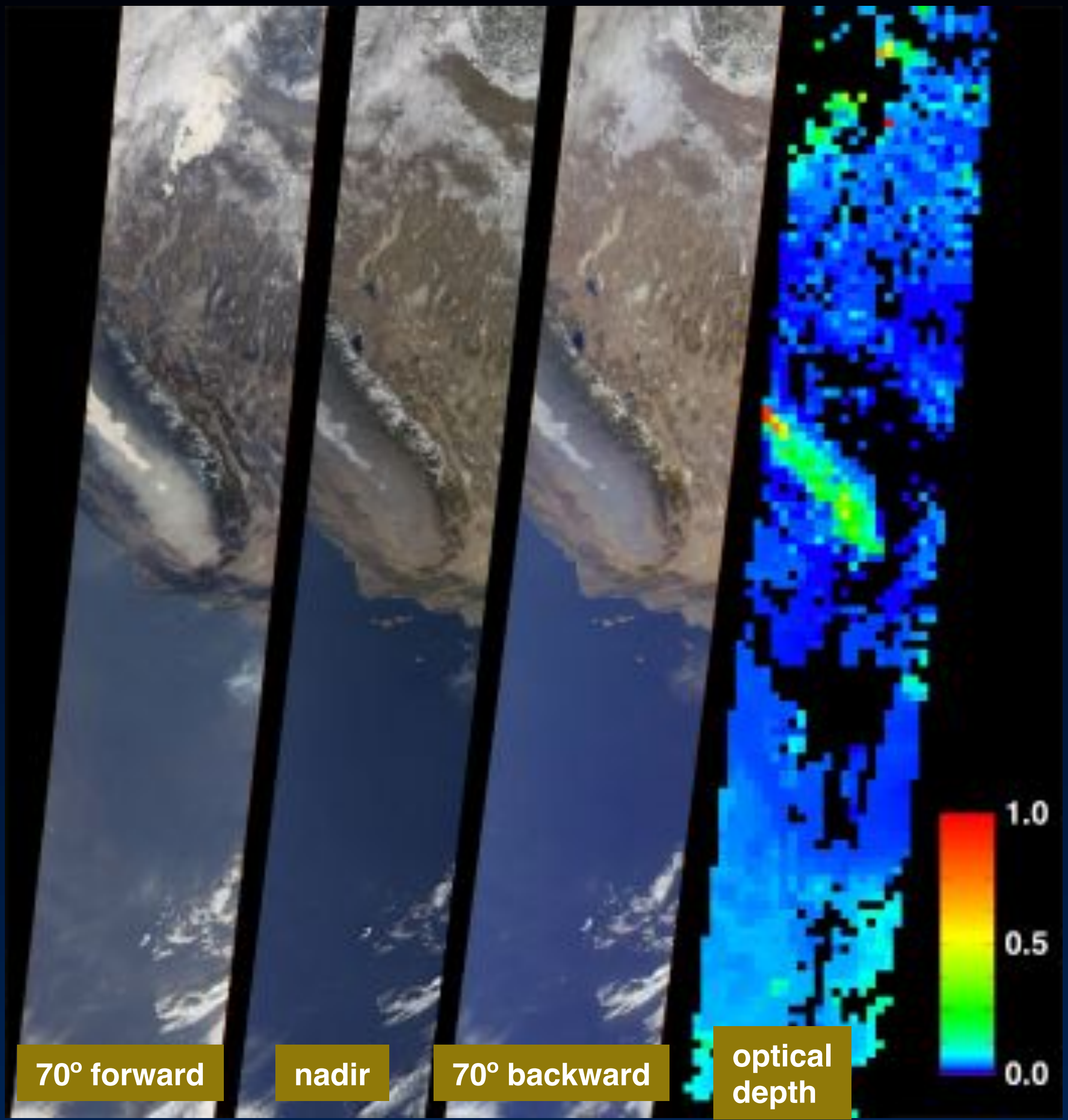

J. Martonchik et al. (2002), TGARS

ATTRIBUTES

- Validation and quality assessment of aerosol optical depth performed
- Validation of aerosol particle properties in progress

  --Angstrom exponent
  --Size binned fractions
  --Single-scattering albedo
  --Sphericity

Southern California and Southwestern Nevada
January 3, 2001

Retrieval of aerosol optical depth over a wide range of surface types

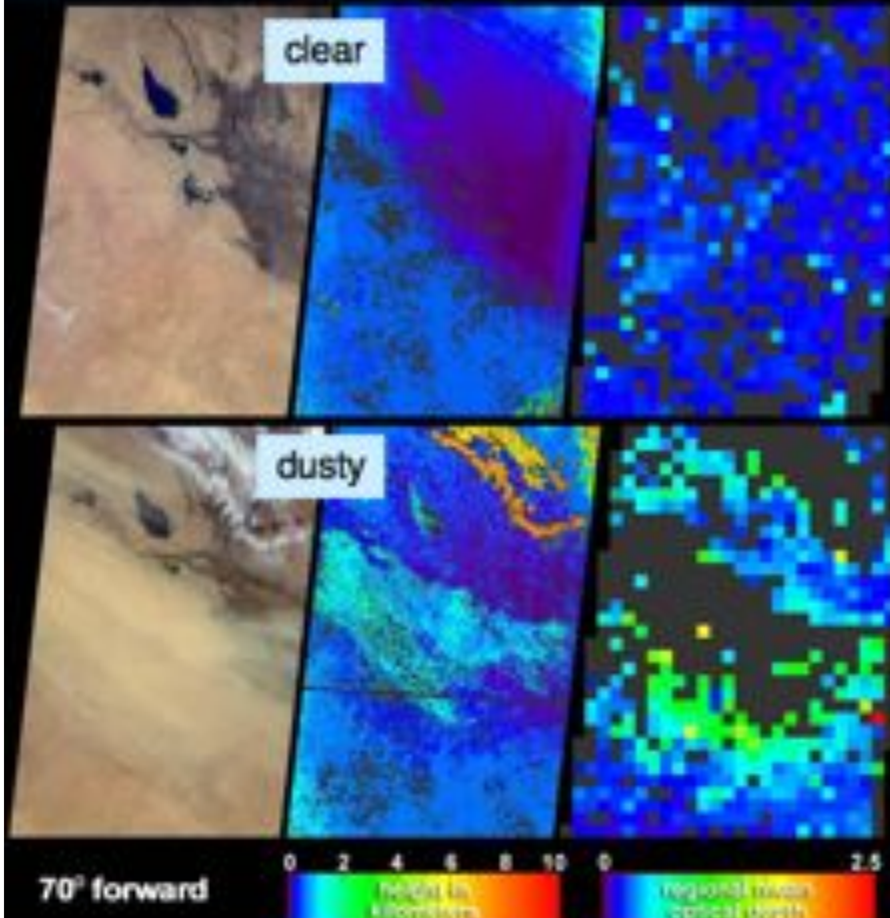

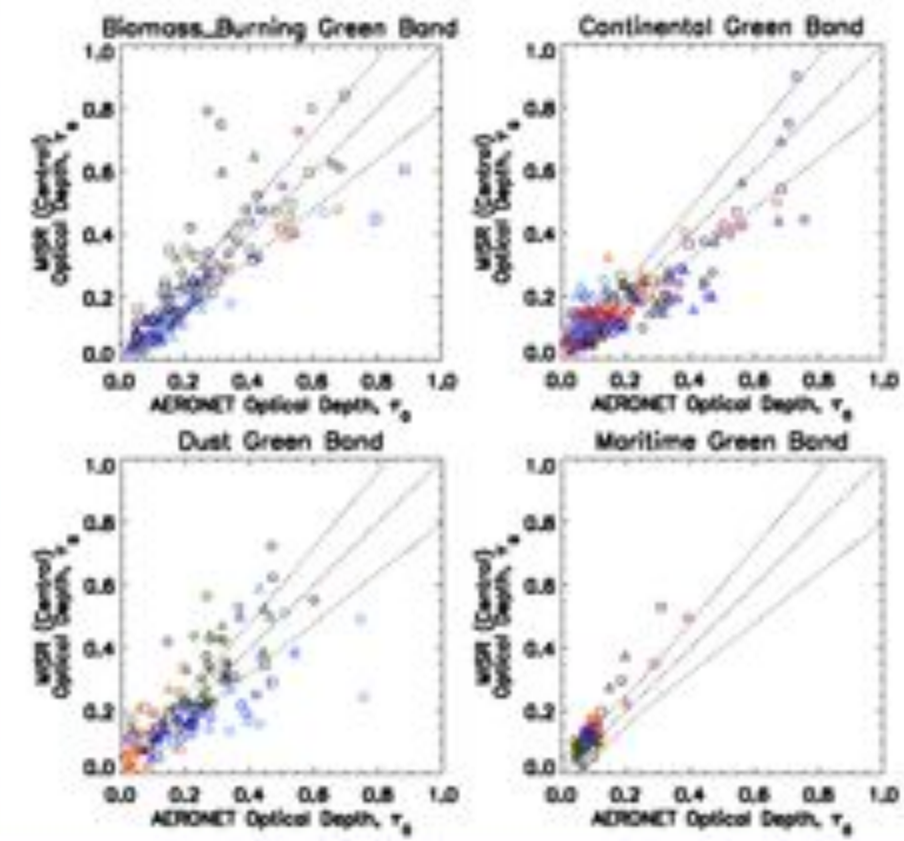

Iraq and Saudi Arabia, April 2004 (top) and May 2004 (bottom)

Global optical depth comparisons With AERONET

MISR sensitivity to aerosol particle properties

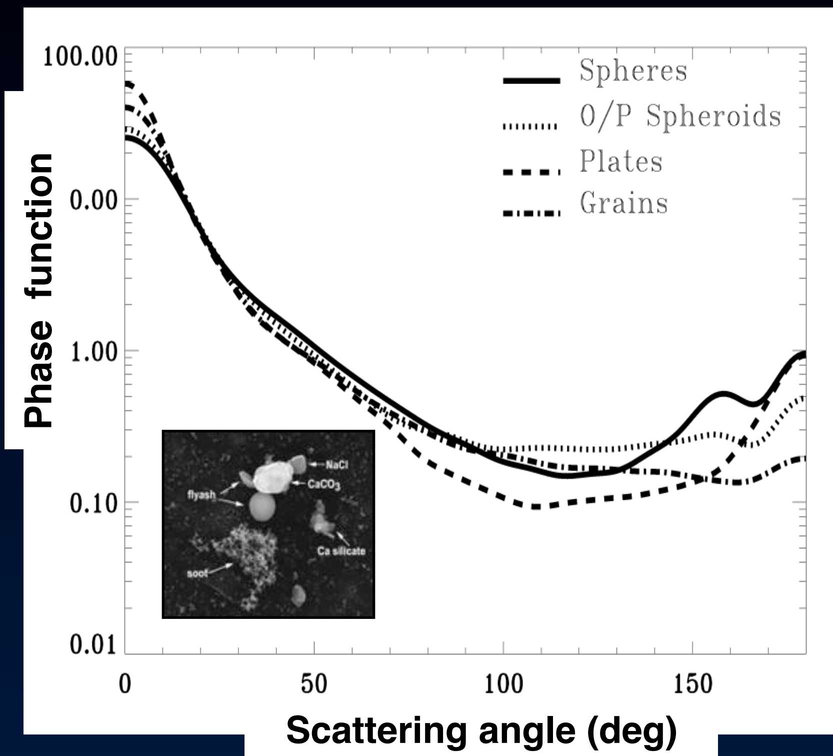

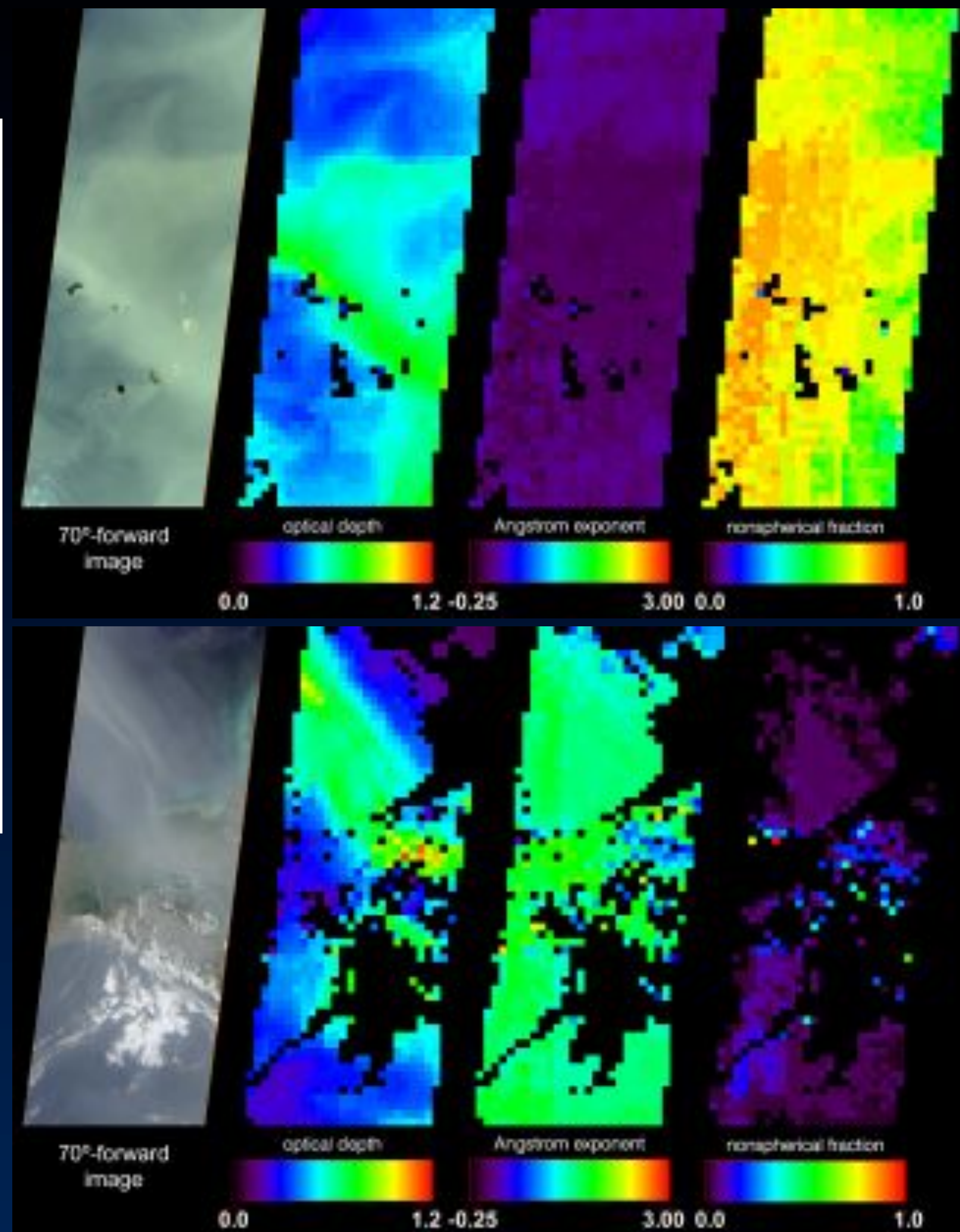

O. Kalashnikova et al. (2005), JGR

Mapping particulate air pollution

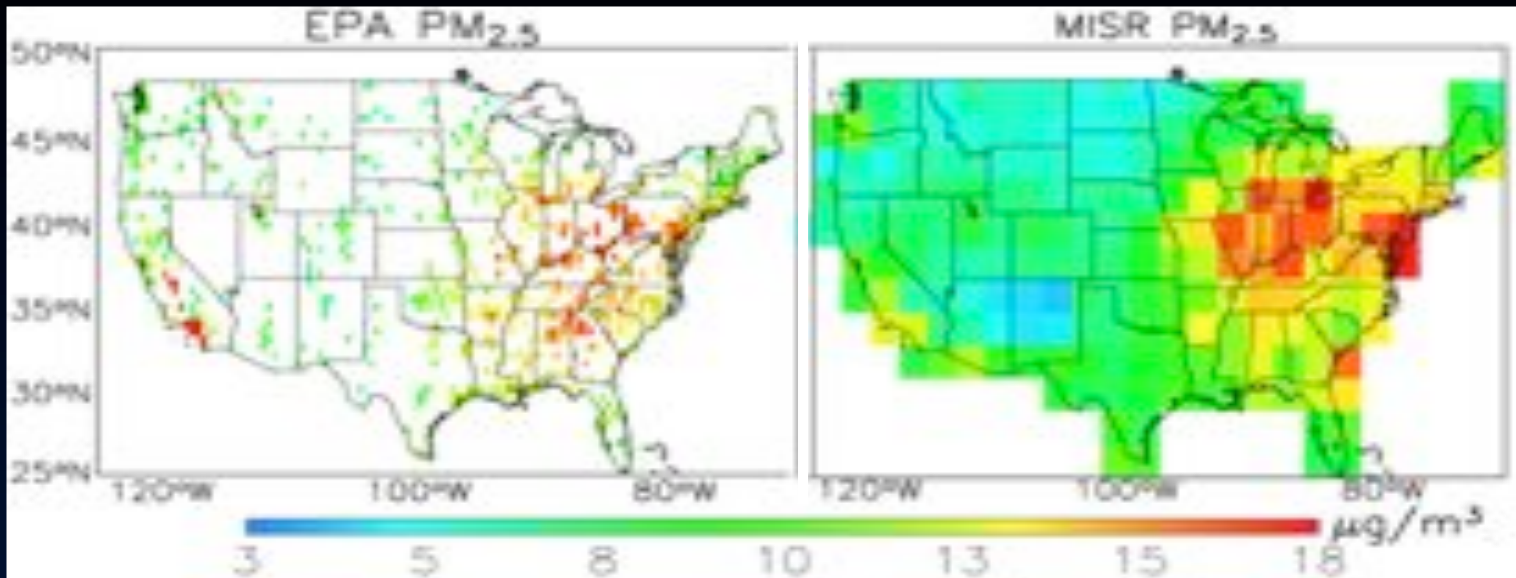

MISR column optical depths are scaled to PM2.5 using a chemical transport model (GEOS-CHEM)

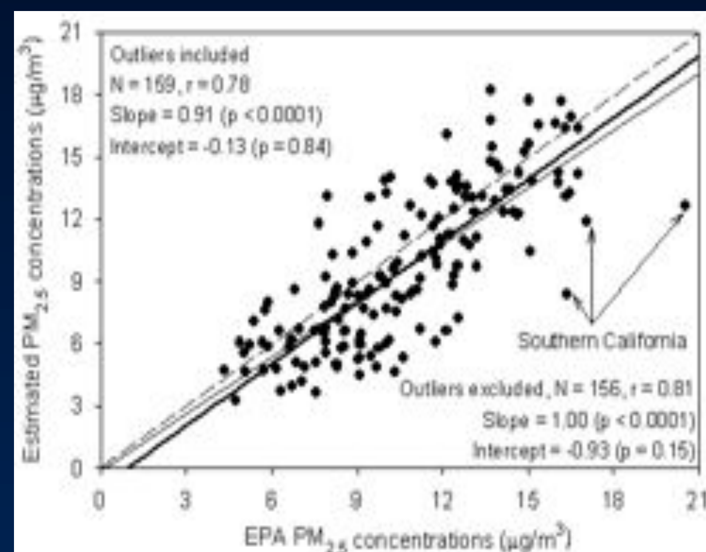

Y. Liu et al. (2005), JGR

L2 Aerosol/Surface Product

Surface parameters

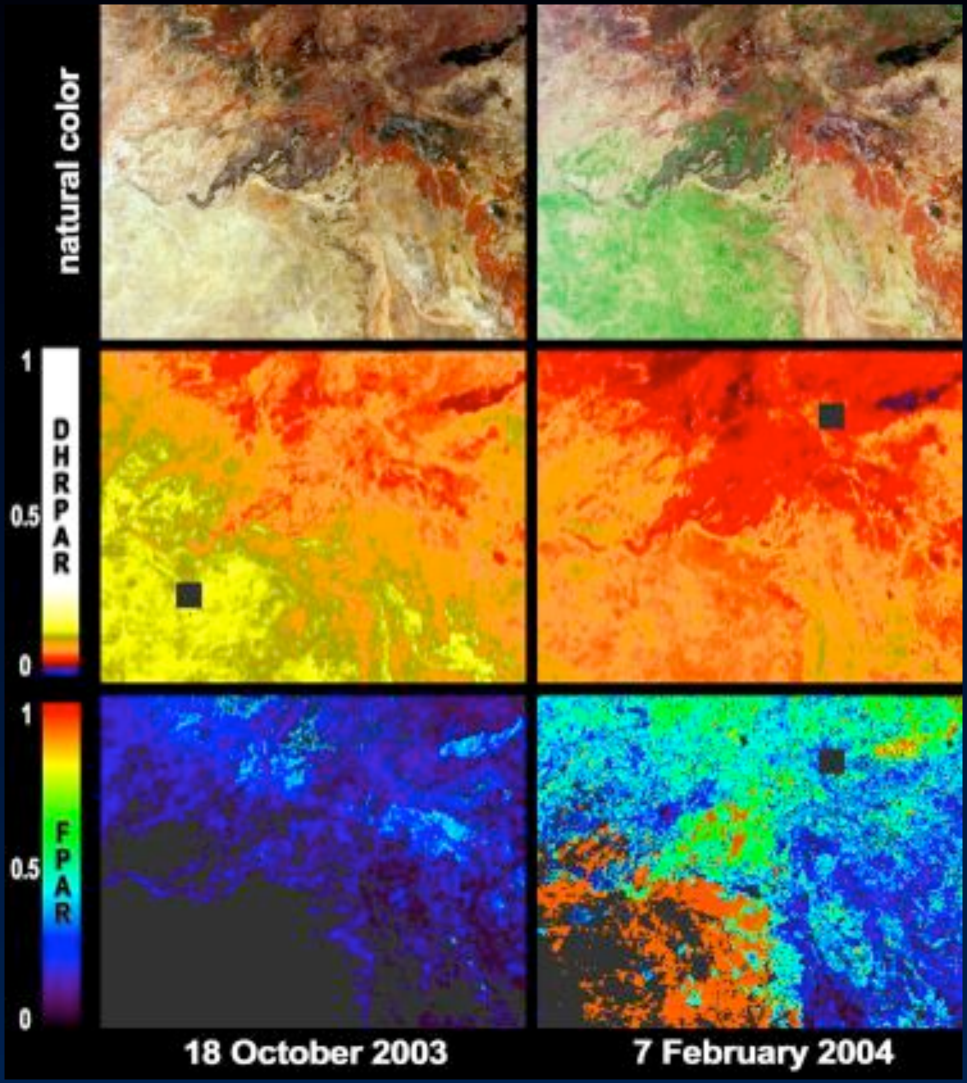

Surface greening from summer rains in Northern Queensland

CONTENTS AND ATTRIBUTES

- Radiometric surface parameters (directional reflectances, albedos)

  Derived from single overpass--no temporal compositing

  Atmospherically corrected

- Vegetation-related quantities (albedo-based surface NDVI, LAI, FPAR)

  LAI-FPAR retrievals are based on 3-D RT models

  Prescribed biome map is not required

- BRF model parameters

Dependence of bidirectional reflectance on surface vegetation subpixel structure: parametric approach

Structurally homogeneous canopy representation composed of finite-sized scatterers

Parametric models
(e.g., Rahman-Pinty-Verstraete function)
$BRF = BRF_0$ * Shape term * Asymmetry term
Shape term = $[\mu\mu_0(\mu+\mu_0)]^{k-1}$

Structurally heterogeneous canopy representation composed of clumped ensembles of finite-sized scatterers

Exponent k establishes whether BRF angular signature gets darker off-nadir (bell-shaped, $k > 1$) or brighter off-nadir (bowl-shaped, $k < 1$)

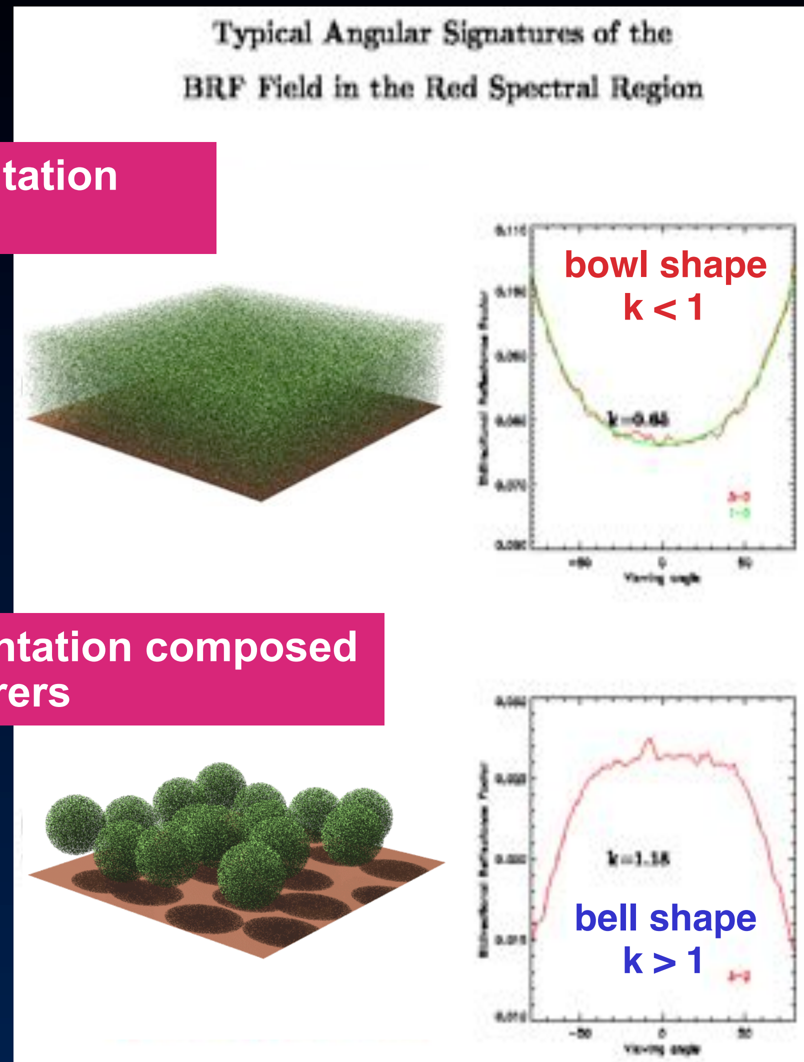

B. Pinty, N. Gobron, J-L. Widlowski, M. Verstraete

Bidirectional reflectances of surface vegetation as observed by MISR

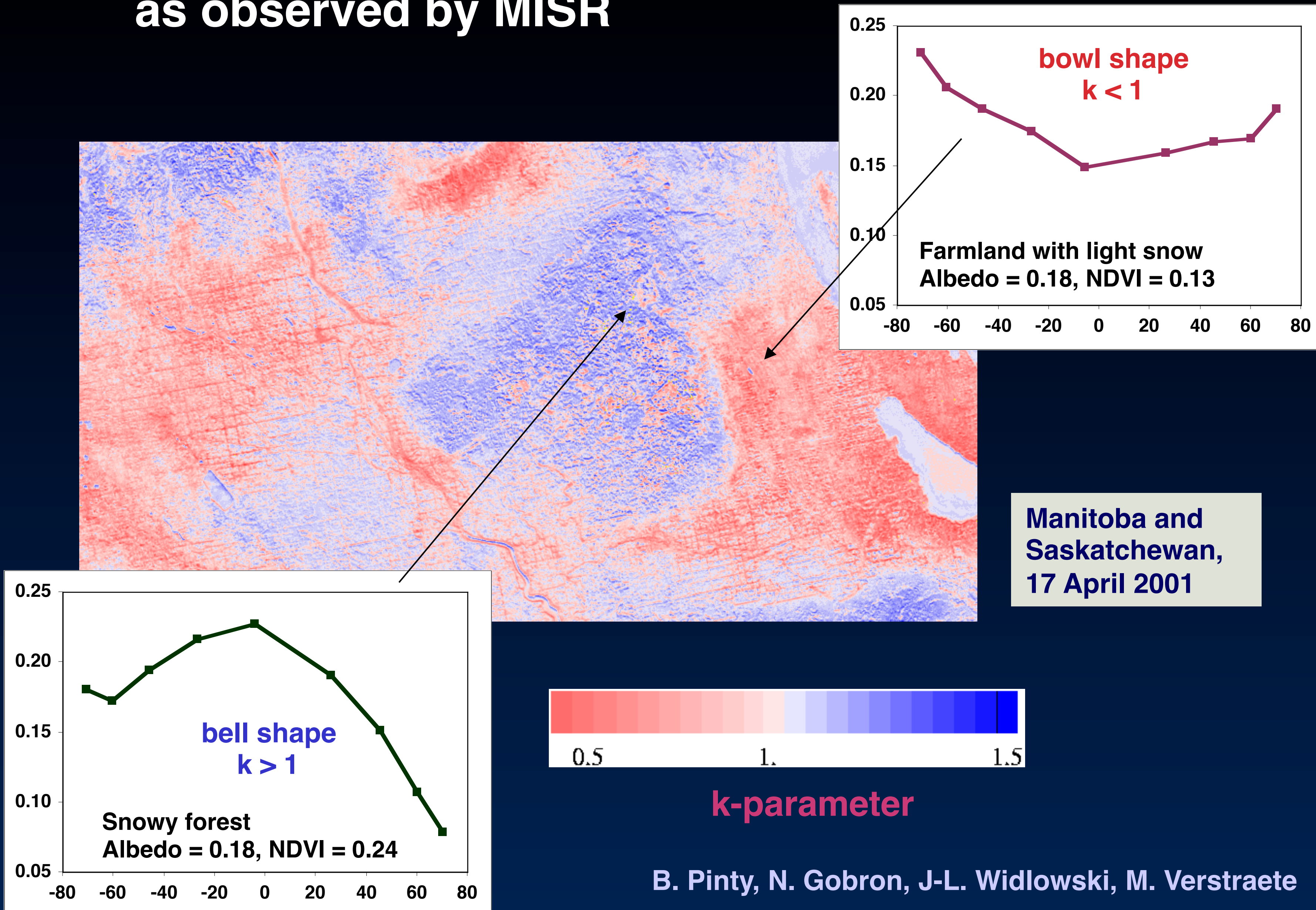

B. Pinty, N. Gobron, J-L. Widlowski, M. Verstraete

Vegetation canopy heights

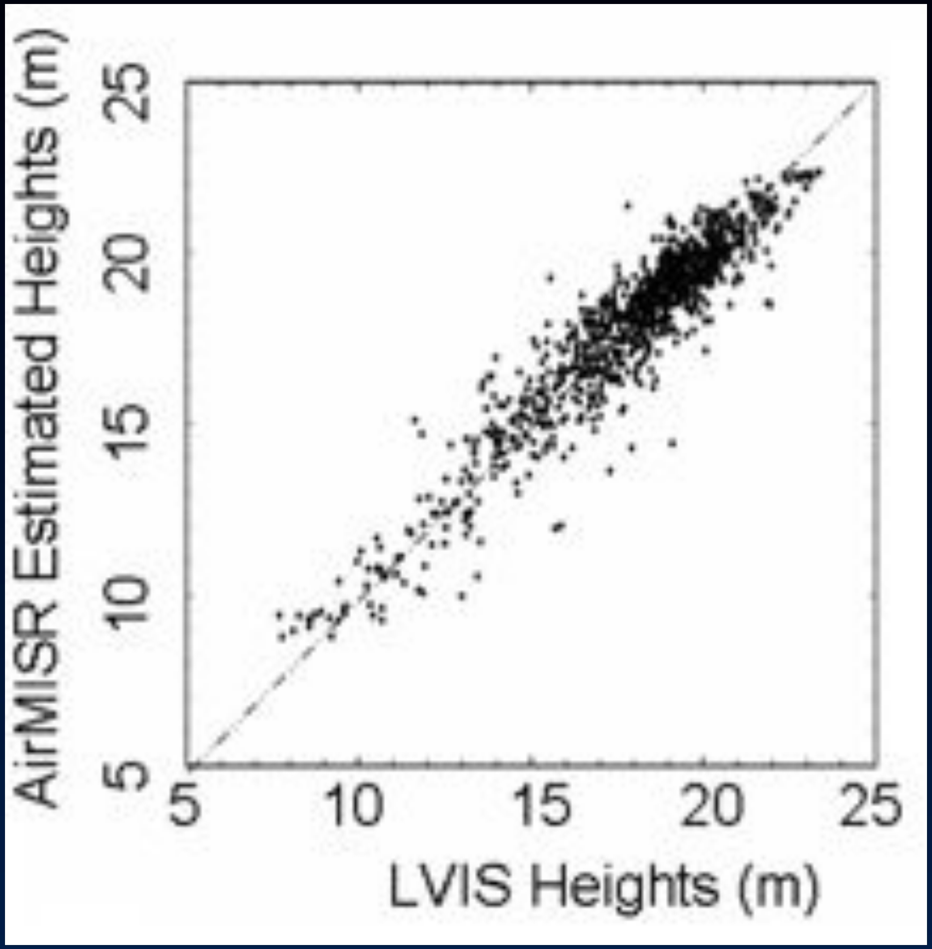

Neural-net derived multiangle height predictor vs. lidar height using airborne (AirMISR/LVIS) data over Maine

Testing with MISR and GLAS is in progress

Kimes et al. (2006), Rem. Sens. Environ.

Mapping of woody shrub encroachment in arid grasslands with MISR

The abundance of woody shrubs in arid grasslands of the southwest US has been changing rapidly, altering carbon and energy fluxes

Strengths of multiangle remote sensing include:

- Sensitivity to vegetation structure, owing to effects of shadowing
- Ability to distinguish canopy and understory reflectance due to contrast differences between nadir and oblique views
- Accuracy improvements in vegetation community and land cover classifications

Looking in the *Backscattering* direction: shadows are HIDDEN

Looking in the *Forward-scattering* direction: shadows are VISIBLE

M. Chopping

Community type classification in arid grasslands

Jornada Experimental Range

- Upland Grasses
- Playa Grasses
- Tarbush
- Mesquite
- Creosotebush
- Other Shrubs
- Not mapped

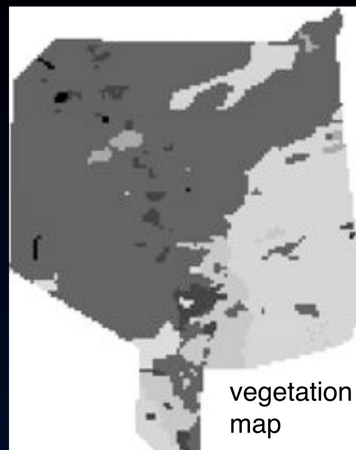

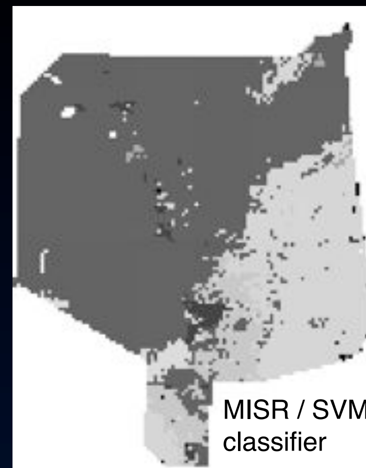

Overall classification accuracy increased from 45% (nadir only) to 77% (with MISR). For 5 of 19 classes, the improvement was 50 percentage points.

Sevilleta National Wildlife Refuge

- Not mapped
- Water or Wet Ground
- Barren or Sparsely Vegetated
- Great Basin Grasslands
- Transition Chihuahuan and Great Basin Grasslands
- Chihuahuan Desert Grasslands
- Transition Chihuahuan and Plains Grasslands
- Plains Grasslands
- Chihuahuan or Great Basin Lowland/Swale Grasslands
- Chihuahuan Desert Creosotebush Shrublands
- Great Basin Shrublands--Fourwing Saltbush/Br. Dalea
- Rocky Mountain Juniper Savanna
- Rocky Mountain Pinyon Woodlands
- Rio Grande Riparian Woodlands

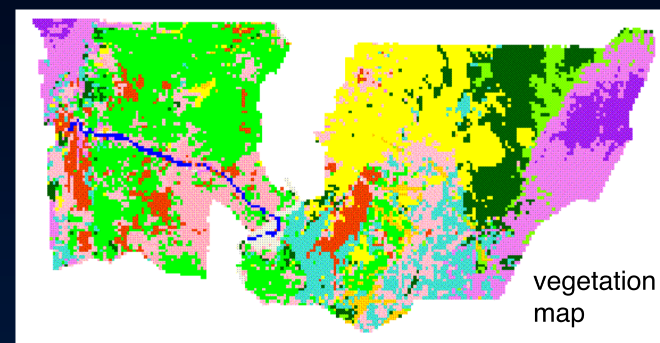

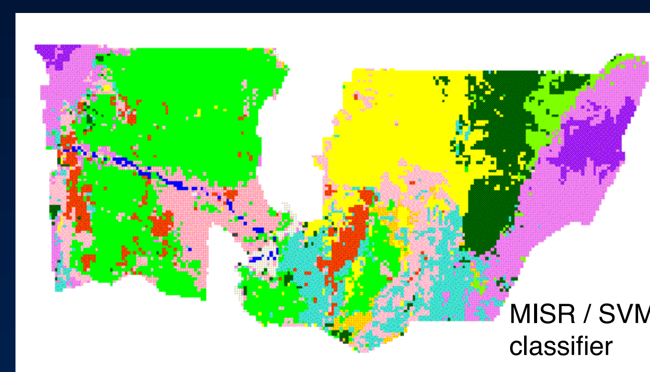

M. Chopping

L3 Gridded Radiances

Means, variances, and covariances

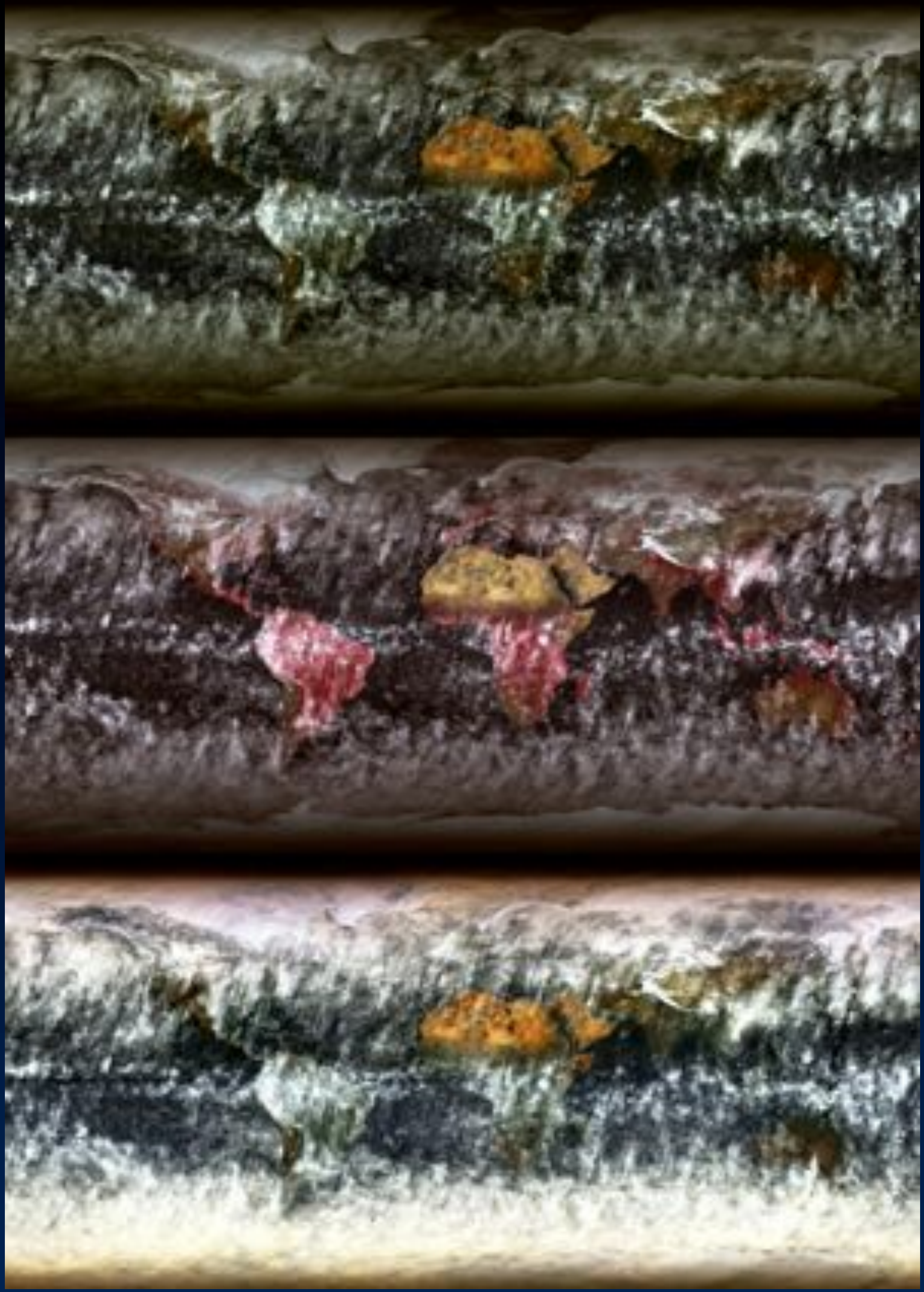

Nadir red, green, blue

Nadir near-infrared, red, green

March 2002

70° forward: red, green, blue (N. hemisphere)
70° backward: red, green, blue (S. hemisphere)

L3 Gridded Height-Resolved Winds

Monthly mean winds August 2005 (0.5-1 km altitude)

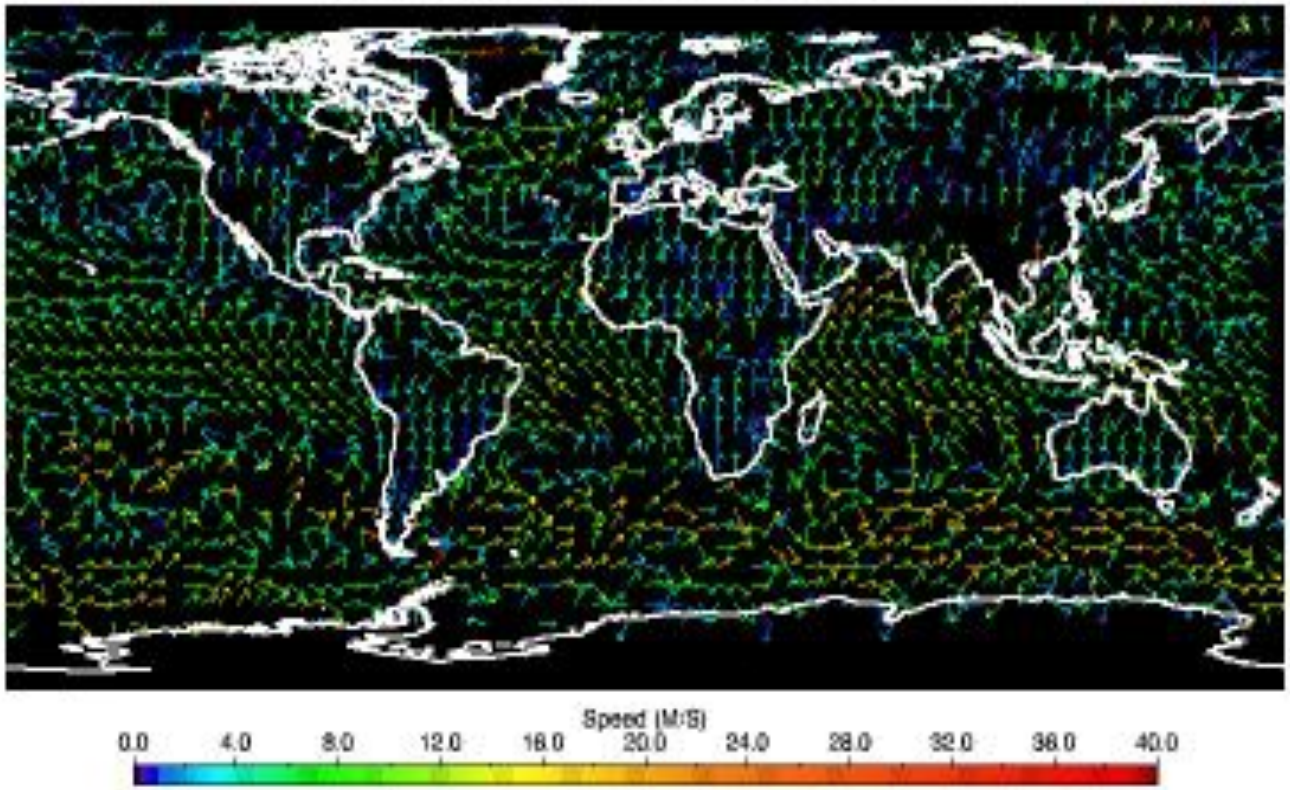

L3 Gridded Aerosol Properties

Global optical depths

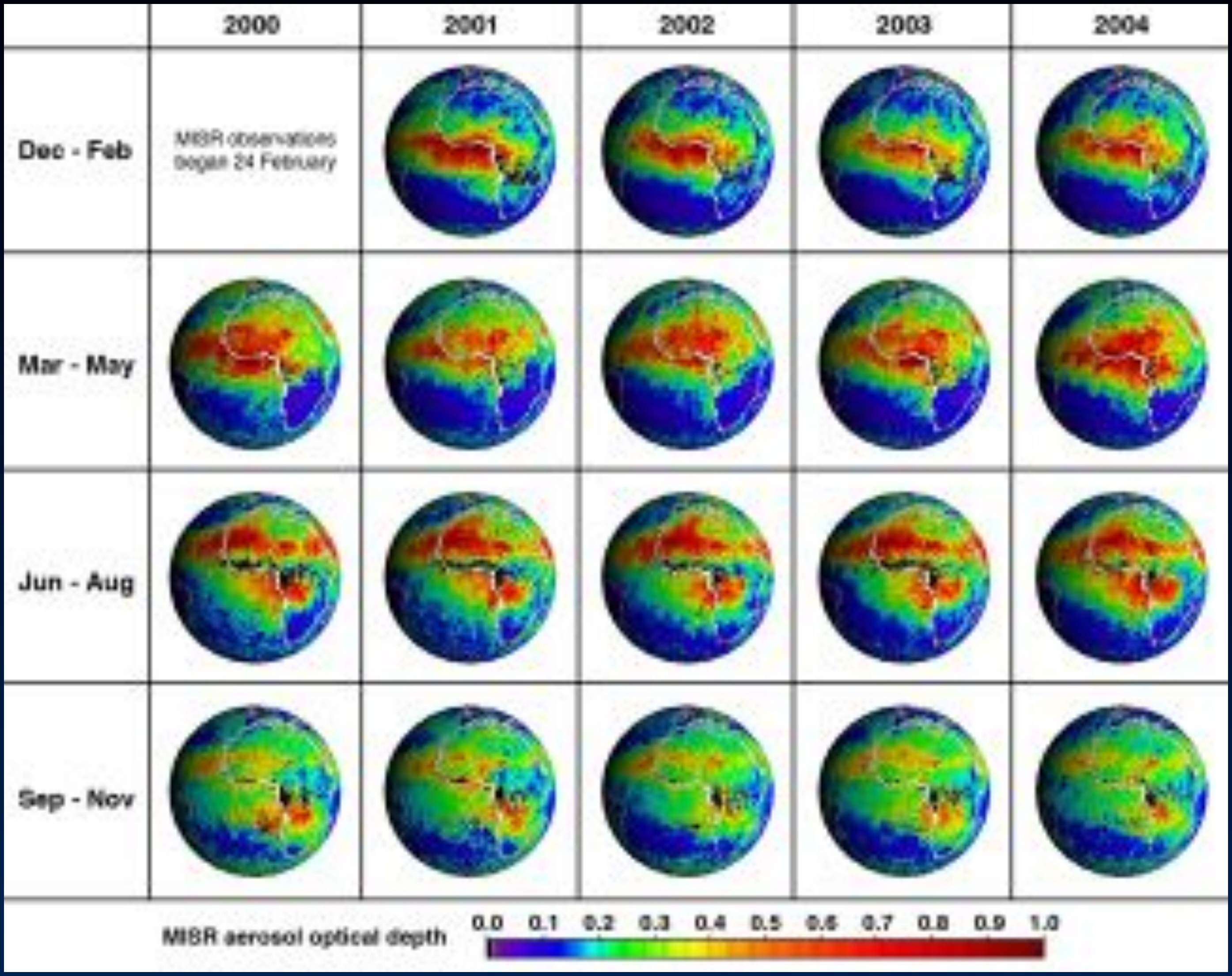

L3 Gridded Surface Properties

Radiative and biogeophysical parameters

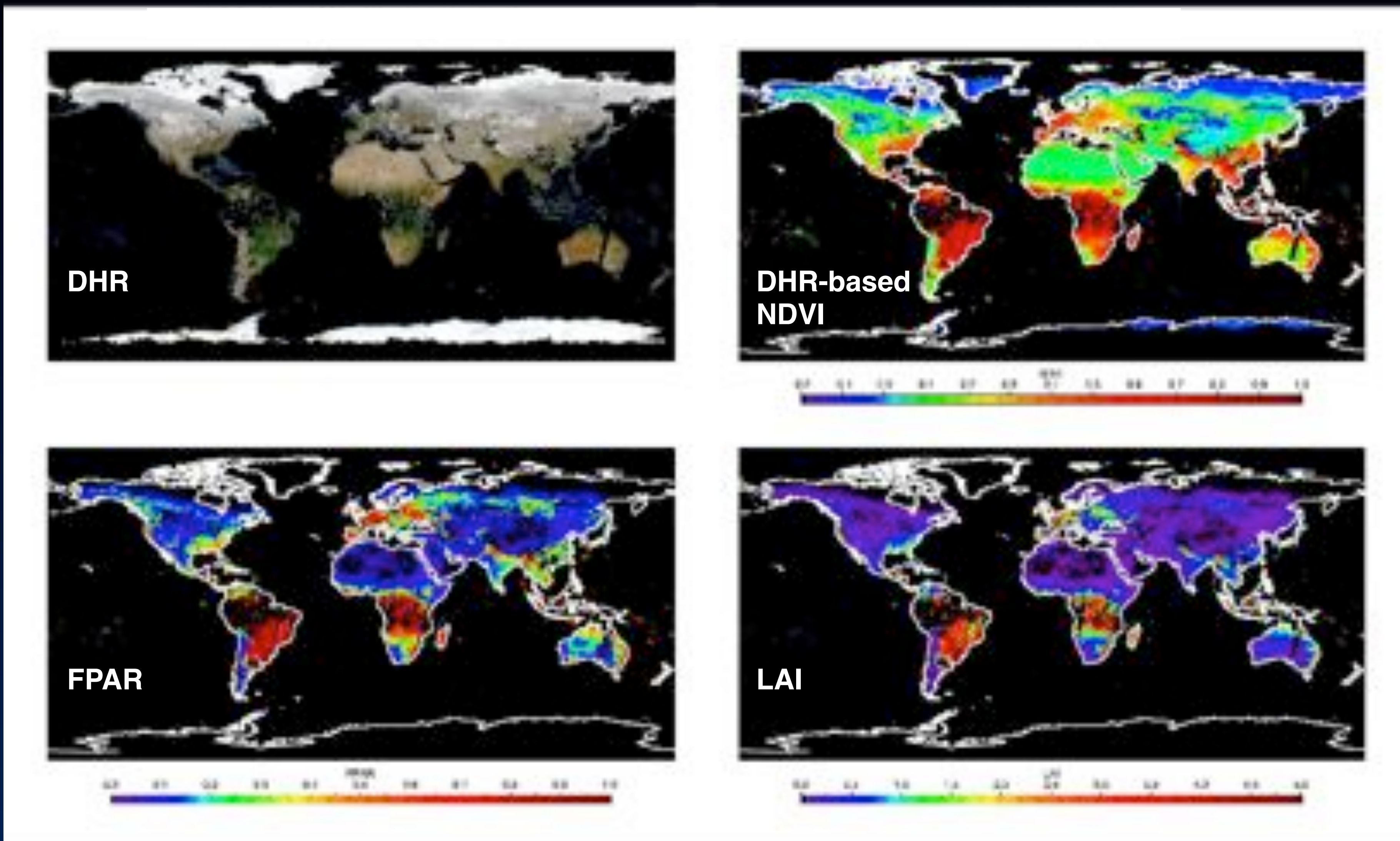

Additional products you might need

Ancillary Geographic Product

--contains latitudes, longitudes, elevations, scene classifiers for each 1.1-km pixel on the Space Oblique Mercator grid

Aerosol Climatology Product

--Aerosol Physical and Optical Properties (APOP) contains characteristics of the component particles used in the aerosol retrievals

--Mixture file contains characteristics of the particle mixtures used

Data quality and maturity levels

Terra data products are given the following maturity classifications:

Beta: Minimally validated. Early release to enable users to gain familiarity with data formats and parameters. May contain significant errors.

Provisional: Partially validated. Improvements are continuing. Useful for exploratory studies.

Validated: Uncertainties are well defined, and suitable for systematic studies.

Mapping of data product maturity to version numbers found at:
eosweb.larc.nasa.gov/PRODOCS/misr/Version/

Be sure to read the quality statements!
eosweb.larc.nasa.gov/PRODOCS/misr/Quality_Summaries/misr_qual_stmts.html

Where to get help and information

LaRC DAAC User Services
larc@eos.nasa.gov

Langley Atmospheric Sciences Data Center DAAC
http://eosweb.larc.nasa.gov

MISR home page
http://www-misr.jpl.nasa.gov

We welcome your feedback and questions!
"Ask MISR" feature on the MISR web site